frontiers | Frontiers in Earth Science

TYPE Original Research
PUBLISHED 18 January 2024
DOI 10.3389/feart.2024.1301999

Check for updates

OPEN ACCESS

EDITED BY
Teresa Drago,
Portuguese Institute for the Sea and Atmosphere, Portugal

REVIEWED BY
Fabienne Marret,
University of Liverpool, United Kingdom
Jonaotaro Onodera,
Japan Agency for Marine-Earth Science and Technology (JAMSTEC), Japan

*CORRESPONDENCE
L. Pérez-Cruz,
perezcruz@igeofisica.unam.mx

†PRESENT ADDRESS
T. W. Höfig,
Project Management Jülich, Jülich Research Centre GmbH, Rostock, Germany

RECEIVED 25 September 2023
ACCEPTED 02 January 2024
PUBLISHED 18 January 2024

CITATION
Velázquez-Aguilar M, Pérez-Cruz L, Urrutia-Fucugauchi J, Marsaglia KM, Coria-Monter E, Monreal-Gómez MA, Teske A, Höfig TW, Aldama-Cervantes A and Jiang SD (2024), Evolution of ocean circulation and water masses in the Guaymas Basin (Gulf of California) during the last 31,000 years revealed by radiolarians and silicoflagellates in IODP expedition 385 sediment cores.
Front. Earth Sci. 12:1301999.
doi: 10.3389/feart.2024.1301999

COPYRIGHT
© 2024 Velázquez-Aguilar, Pérez-Cruz, Urrutia-Fucugauchi, Marsaglia, Coria-Monter, Monreal-Gómez, Teske, Höfig, Aldama-Cervantes and Jiang. This is an open-access article distributed under the terms of the Creative Commons Attribution License (CC BY). The use, distribution or reproduction in other forums is permitted, provided the original author(s) and the copyright owner(s) are credited and that the original publication in this journal is cited, in accordance with accepted academic practice. No use, distribution or reproduction is permitted which does not comply with these terms.

Evolution of ocean circulation and water masses in the Guaymas Basin (Gulf of California) during the last 31,000 years revealed by radiolarians and silicoflagellates in IODP expedition 385 sediment cores

M. Velázquez-Aguilar[1], L. Pérez-Cruz[2,3]*, J. Urrutia-Fucugauchi[2,3], K. M. Marsaglia[4], E. Coria-Monter[5], M. A. Monreal-Gómez[5], A. Teske[6], T. W. Höfig[7†], A. Aldama-Cervantes[1] and S. D. Jiang[8]

[1]Posgrado en Ciencias del Mar y Limnología, Universidad Nacional Autónoma de México, México City, México, [2]Instituto de Geofísica, Universidad Nacional Autónoma de México, México City, México, [3]Instituto de Investigación Científica y Estudios Avanzados Chicxulub, Parque Científico y Tecnológico de Yucatán, Mérida, México, [4]Department of Geological Sciences, California State University, Northridge, CA, United States, [5]Instituto de Ciencias del Mar y Limnología, Universidad Nacional Autónoma de México, México City, México, [6]Department of Marine Sciences, University of North Carolina at Chapel Hill, Chapel Hill, NC, United States, [7]International Ocean Discovery Program, Texas A&M University, College Station, TX, United States, [8]Institute of Groundwater and Earth Sciences, Jinan University, Guangzhou, China

The high-resolution analysis of radiolarians and silicoflagellates in sediments from Holes U1545A and U1549A drilled during IODP Expedition 385 in the Guaymas Basin, in the Gulf of California provides detailed insights into the evolution of ocean circulation and water masses, and its relation to Eastern Tropical Pacific Ocean climate conditions, over the past 31,000 cal years BP (based on AMS radiocarbon dates). In the pre-Last Glacial Maximum, the Guaymas Basin experienced alternating circulation patterns of California Current Water (CCW) and Gulf of California Water (GCW), with an extended presence of the Pacific Intermediate Water (PIW) owing to: amplified jet streams; southern movement of the California Current System (CCS) and the incursion of CCW into the gulf; and increased North Pacific Intermediate Water (NPIW) formation. The Last Glacial Maximum witnessed the incursion of CCW due to the stronger CCS. The dominance of the PIW indicates the expansion and formation of NPIW. The Heinrich-I event as manifested in the core record, displays two distinct patterns, one suggesting GCW-like dominance and the other, the occurrence of CCW. The Bølling-Ållerød interstadial featured the entry of Tropical Surface Water (TSW), GCW, and CCW, linked with the northward migration of the Intertropical Convergence Zone. In the Younger Dryas, CCW dominated, transitioning to GCW as colder climatic conditions and more intense CCS. The Holocene

displayed alternating periods of TSW and GCW, with a modern monsoon regime from 7,600 to 1,000 cal years BP. From 1,000 cal years BP to the present the ITCZ shifted to the south.

KEYWORDS

hydrographic structure, water masses, Guaymas Basin, radiolarians, silicoflagellates, International Ocean Discovery Program expedition 385, late quaternary

1 Introduction

The sedimentary records in the Gulf of California (GoC), and in particular in the Guaymas Basin (GB), play a crucial role in paleoceanographic and paleoclimatic studies because of the unique setting that allows the preservation of high-resolution sedimentary sequences, providing valuable insights into past environmental changes (e.g., Barron et al., 2005; McClymont et al., 2012). The sensitivity of the GB to regional variations in the gulf and the larger-scale climate circulation of the Eastern Tropical Pacific Ocean (ETPO) makes its sediment record an ideal proxy for unraveling regional and global climatic shifts (e.g., Barron et al., 2005), plus tectonic dynamics contribute to sedimentary variations reflecting changes in sea level, ocean circulation, and local geological processes (Lizarralde et al., 2007; Miller and Lizarralde, 2013).

Key paleoclimatic changes in the GB over the late Quaternary have revealed significant insights through multiproxy analyses, including stable isotopes, biomarkers, and microfossil assemblages, that offer understandings into sea surface temperature (SST) changes, surface and subsurface circulation, productivity, and precipitation regimes. In particular, studies of climatic variability across the GB have covered mainly the last ~20,000 cal years BP at different timescales (e.g., Keiwin and Jones, 1990; Sancetta, 1995; Pride et al., 1999; Barron et al., 2005; McClymont et al., 2012); however, some studies extend further to ~50,000 cal years BP (Price et al., 2012; Cheshire and Thurow, 2013; Barron et al., 2014). Paleoclimatic reconstructions are based on several proxies (e.g., microfossils, opal, TOC, stable isotopes of $\delta^{18}O$ and $\delta^{15}N_{org}$, molecular $U^{37}K'$ and $TEX^{86}H$ indexes, and reflectance) to identify changes in ocean productivity, wind-driven upwellings, as well as shifts in water column oxygenation and SST. Barron et al. (2014) suggested warm and stratified conditions during MIS 3 in the GB, in contrast to the presence of cold (SST <16°C) and low-salinity water during MIS 2. The included Heinrich Events (HE 3, 2, and 1) were characterized by low-productivity conditions due to diminishing upwelling because of the weakening of northwesterly winds (Price et al., 2012). During the Last Glacial Maximum (LGM), it has been suggested that productivity decreased, and precipitation increased, due to the latitudinal migration of the North Pacific High (NPH) and the polar jet stream, towards their southern position (Cheshire and Thurow, 2013); however, in model simulation studies these conditions are not observed (McClymont et al., 2012). Around 16,500 cal years BP, a cold episode was defined, characterized by increased precipitation and surface waters with low salinity in the GB (Keiwin and Jones, 1990). This suggests weakened northwesterly winds and subtropical water incursions into the GoC, causing changes in the extent of subsurface waters and diminishing upwelling and mixing processes (Pride et al., 1999). In the GB during the Bølling-Ållerød (B/A), alternating periods of eutrophic and oligotrophic conditions have been recognized with a sudden increase in SST of 3°C recorded at ~13,000 cal years BP (McClymont et al., 2012). The Younger Dryas was identified as a transitional event with highly oxygenated intermediate waters in the GoC (Keiwin and Jones, 1990), low productivity, and conditions similar to those developed during El Niño Southern Oscillation (ENSO) (Barron et al., 2005), as well as an increase in the GB SST (McClymont et al., 2012; Price et al., 2012). Records of SST suggest a warm climate during the Holocene (SST >24°C) and, in general, high productivity (Douglas et al., 2007). Furthermore, the modern east-west contrast in productivity in the GoC began between ~6,200 and 5,400 cal years BP, associated with the onset of the North American Monsoon (NAM) system (Barron et al., 2005). Also, changes in the SST were identified at ~10,000 cal years BP and ~8,200 cal years BP and linked to the migration of the Intertropical Convergence Zone (ITCZ) and the NPH (McClymont et al., 2012) to the north.

Although several paleoceanographic studies have been developed in this region, understanding the hydrographic structure of the GoC and processes forcing changes still needs to be well resolved. It is crucial to unravel how the Pacific Ocean dynamic and global climate have influenced the gulf to decipher the intricate relationship between the ETPO and the GoC, which in turn will shed light on climatic evolution during the late Quaternary. High-resolution proxy data are also required to allow constrained models and enhance their accuracy.

This study focuses on siliceous microfossils—polycystine radiolarians (hereafter referred to as radiolarians) and silicoflagellates—to reconstruct hydrographic structure, water masses, and circulation patterns in the GB during the past 31,000 cal years BP.

Radiolarians are widely distributed in the ocean, dwelling in shallow and deep environments associated with different water masses and their corresponding physical-chemical properties (e.g., temperature, salinity, nutrients) (Molina-Cruz et al., 1999; Boltovskoy et al., 2010), and silicoflagellates are particularly abundant in nutrient-rich, upwelling areas (Schrader et al., 1986; Barron et al., 2014), and reflect changes in SST (Barron et al., 2004). Although proxies have distinct sensitivities and limitations, silicoflagellates and shallow-dwelling radiolarians respond similarly to specific physical and chemical environmental changes. Thus, these proxies may be jointly considered when interpreting climate variations over time. Here, we present high-resolution records of radiolarian assemblages and silicoflagellates to (1) investigate hydrographic and climatic changes on glacial-interglacial, millennial, and sub-millennial timescales and (2)

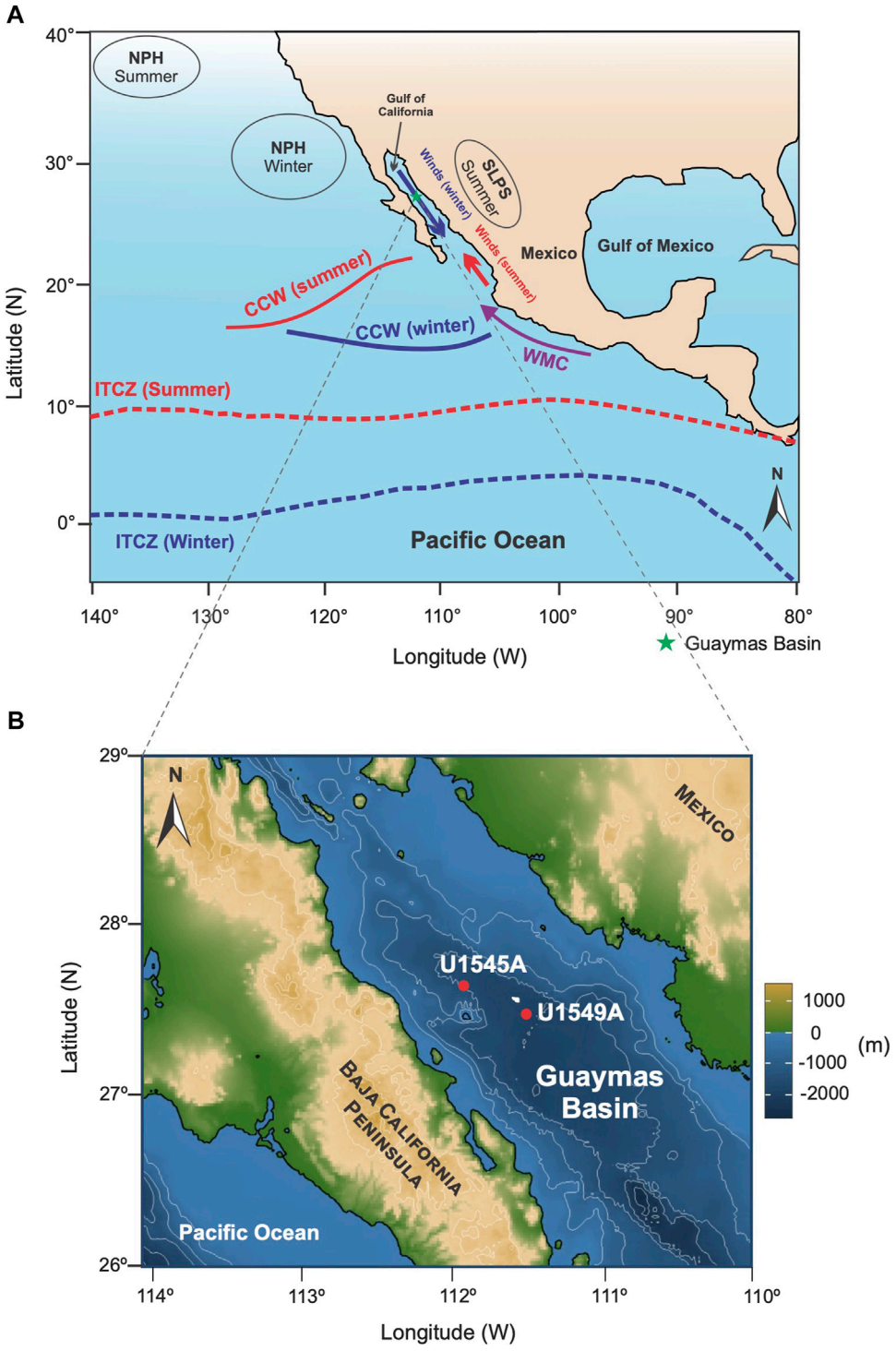

FIGURE 1
(A) Map showing the position of atmospheric centers and ITCZ position during summer and winter. Winds direction in the Gulf of California is shown in bold arrows. NPH, North Pacific High; SLPS, Sonora Low Pressure Center; CCW, California Current Water; WMC, West Mexican Current. Continuous bold lines represent the southern limit of the California Current System (CCS) during summer and winter (Kessler, 2006), **(B)** Location of sampled drilling sites U1545A and U1549A.

establish the links of the regional hydrographic settings to the ETPO. Understanding the occurrence of water masses in the past will expand the knowledge about oceanographic dynamics and its relationship with regional and global climatic variability.

1.1 Study area

The GoC is an inland sea in the ETPO (22–32°N, 105 to 115°W). It is 1,130 km long, and its width ranges from 80 to

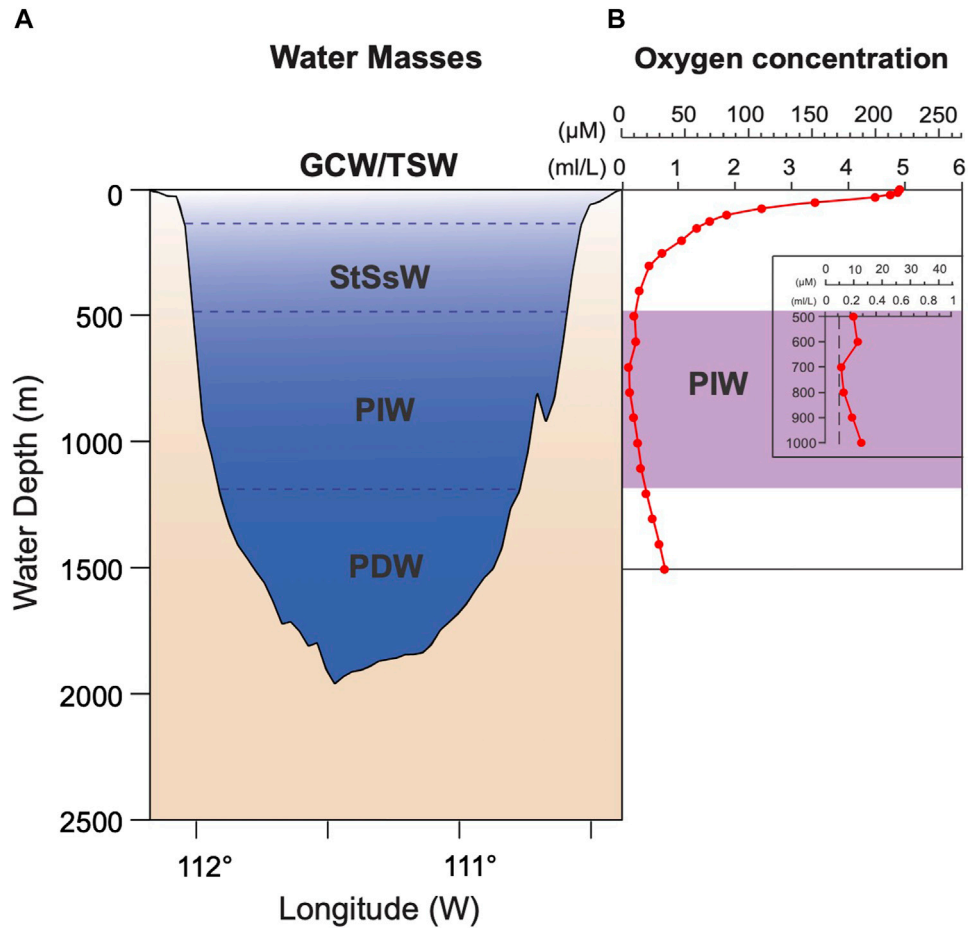

FIGURE 2
(A) Water masses in the Guaymas Basin: GCW, Gulf of California Water; TSW, Tropical Surface Water; StSsW, Subtropical Subsurface Water; PIW, Pacific Intermediate Water; PDW, Pacific Deep Water (Lavin et al., 2009). **(B)** Dissolved oxygen concentration in Guaymas Basin (García et al., 2006).

200 km (Lavin and Marinone, 2003) (Figure 1A). The GB is located in the central GoC (27°–28°N, 111°–112°W) (Figure 1B); it is an elongate semi-enclosed basin formed by seafloor spreading since ~6 Ma (Lizarralde et al., 2007; Miller and Lizarralde, 2013) with water depths up to 2000 m (Figure 2A) (Bray, 1988; Stock and Hodges, 1989; Lavin and Marinone, 2003; Lizarralde et al., 2007).

1.1.1 Climate setting

The hydrographic structure and circulation in the GoC are imposed mainly by the ETPO dynamic (Figure 1A) (Amador et al., 2006; Lavin et al., 2009; Lavín et al., 2014). The surface circulation is driven by seasonal climate variability (Amador et al., 2006; Lavin et al., 2009) in response to insolation and atmospheric changes that control the position of the NPH system, the wind and precipitation patterns (NAM), and the latitudinal migration of the ITCZ (Figure 1A) (Amador et al., 2006). These processes affect the pycnocline topography, thermocline depth, and the circulation of surface currents extending to the northern GoC, such as the California Current System (CCS) and the West Mexican Current (WMC) (Kessler, 2006; Lavín et al., 2014) (Figure 1A). Circulaton of the surface and subsurface water masses and the ocean dynamic in the GoC result from a net exchange of water with the Pacific Ocean, characterized by the outflow of 0–200 m surface water, inflow of 200–600 m subsurface water (Bray, 1988; Álvarez-Borrego, 2010), and by significant influence of the mesoscale geostrophic gyres (Lavín et al., 2014).

The climate in the GoC is markedly seasonal, with two well-defined phases. During the winter-spring phase, the insolation in the Northern Hemisphere is low at ~225 W/m^2 (De Menocal et al., 2000), and the ITCZ migrates southwards and approaches the equator (~2°N) (Figure 1A) (Koutavas and Lynch-Stieglitz, 2005; Amador et al., 2006; Schneider et al., 2014). In the GoC, NW winds predominate (Lavin et al., 2009) and induce the transport of surface water along the eastern margin flowing out of the gulf enhancing wind-driven upwelling (Badan-Dangon et al., 1991), decreasing the SST, promoting a broader mixed layer and the weakening of the thermocline (Marinone, 2003; Douglas et al., 2007). In the summer-fall phase, insolation in the Northern Hemisphere is at its maximum at ~450 W/m^2 (De Menocal et al., 2000; Douglas et al., 2007), the ITCZ reaches its northernmost latitude located at ~9°N (Figure 1A) (Koutavas and Lynch-Stieglitz, 2005; Schneider et al., 2014), and the SE winds strengthen (Lavin et al., 2009). In this phase, the temperature, humidity, and precipitation increase.

TABLE 1 Water masses in the GoC.

Water mass	Abbreviation	Salinity (g kg−1)	Temperature (°C)	Depth (m)
Tropical Surface Water	TSW	<34.6	>25.1	0—50*
Gulf of California Water	GCW	>35.1	>12	0—150*
California Current Water	CCW	<34.6	10–21	0—150*
				0—500**
Subtropical Subsurface Water	StSsW	34.6–35.1	9–8	75—400*
Pacific Intermediate Water	PIW	34.6–34.9	4–9	400—1,200***
Pacific Deep Water	PDW	34.5–34.7	4	>1,200***

*Portela et al, 2016, **Castro et al., 2017, ***Lavín et al., 2009.

1.1.2 Water masses and surface ocean circulation

Water masses exchange with the Pacific through the mouth of the GoC, linking ETPO conditions to the GoC climate. In the GB, several water masses have been identified (Figure 2A; Table 1): the Pacific Deep Water (PDW), the Pacific Intermediate Water (PIW), the Subtropical Subsurface Water (StSsW), the Tropical Surface Water (TSW), and the Gulf of California Water (GCW); the latter originates by mixing of TSW with StSsW and evaporation processes inside the gulf (Lavin and Marinone, 2003; Lavin et al., 2009; 2014; Portela et al., 2016). In addition, California Current Water (CCW) has been identified in the mouth of the GoC (Lavin et al., 2009). Most of these water masses originate in the Pacific Ocean, except for the GCW, which forms inside the gulf. Several factors, including ocean circulation, climate, and bathymetry, influence them. Low oxygen concentrations at intermediate depths are characteristic of the GoC waters (e.g., Roden, 1964; Alvarez-Borrego and Lara-Lara, 1991). The concentration of oxygen at intermediate depths (~500–1,100 m) is less than 0.1 mL/L (e.g., García et al., 2006; Figure 2B).

The GB surface ocean circulation is driven by seasonal patterns. During the winter (Lavin and Marinone, 2003), NW winds cause a southward migration of the thermohaline front toward the mouth of the gulf. Thus, the flow of the TSW into the gulf decreases (Lavín et al., 2014; Portela et al., 2016), and evaporation conditions in the northern basin promote the formation of the GCW that flows south along the eastern margin of the gulf (Bray, 1988), while the CCW flows into the gulf along its southwestern margin (Portela et al., 2016). In the summer, TSW is transported toward the gulf strengthened by the SE winds, with enhanced upwelling on its western margin, and SST increased (Marinone, 2003). The warm surface waters cover the central and southern regions of the gulf, forming a deep thermocline, and the nutrient advection to the surface is delayed, thus decreasing the primary productivity (Álvarez-Borrego and Lara-Lara, 1991).

2 Materials and methods

2.1 Sediment cores

For this study, we analyzed sediment core samples obtained aboard of the deep-sea drill ship *JOIDES Resolution* during the International Ocean Discovery Program (IODP) Expedition 385 to the GB from September to November 2019. We focus on two sites (U1545-and U1549) and specifically cores recovered from the first (A) hole drilled at each site (Figure 1B). Hole U1545A is located on the lower slope off Baja California in the northwestern part of the GB (lat. 27°38.2325′N, long. 111°53.3406′W) in a water depth of 1,593.5 m. It was drilled to 503.3 m below seafloor (mbsf), corresponding to a curated core depth of 507.27 mbsf (Teske et al., 2021a), and for this study, we analyzed the uppermost first 41 m of sediments (Cores 385-U1545A-1H to 5H). Hole U1549A is located in the central-western part of the GB (lat. 27°28.3317′N, long. 111°28.7844′W), in a water depth of 1840.07 m; it was drilled to 168.0 mbsf, which corresponds to a curated core depth of 168.35 mbsf (Teske et al., 2021b), and we studied the uppermost 28 m of sediments (Cores 385-U1549A-1H to 4H).

2.2 Lithology

Sediments cored in Hole U1545A are mostly laminated diatom ooze and clay-rich diatom ooze, with laminae alternating between biogenic-particle-dominated (mainly diatom ooze) and terrigenous-particle-dominated (mainly clay minerals with minor siliciclastic silt) end members; the presence of lamination suggests that the hemipelagic sediments were deposited in suboxic to anoxic seafloor conditions (Teske et al., 2021b).

Sediments recovered in Hole 1549A, are mainly diatom ooze and clay-rich diatom ooze; however, from ~18 to 14 m subseafloor depth (Sections 385-U1549A-3H-2, 3H-1, 2H-7, and 2H-6; Supplementary Figure S1), there is a thick depositional layer rich in terrigenous siliciclastic particles above a base marked by silt-to-sand-sized bioclasts (foraminifers and bivalves) and terrigenous debris. This layer correlates with tilted laminae (from Cores 385-U1549A-2H to 3H) owing to slope instability and mass-gravity flow and deposition (Teske et al., 2021a). Considering that a climatic signal would not have been recorded in this relatively instantaneously deposited event bed, samples were not taken for analysis from this interval.

2.3 Chronology and time frame

In the absence of microfossils (foraminifera), owing to their limited presence and/or preservation, bulk sediment radiocarbon

dating by the accelerator mass spectrometry (AMS) technique is the most common approach and most appropriate for young, well-buried, capped, undisturbed sediments (Jull, 2007). Samples for radiocarbon dating were selected along the studied cores considering the sedimentation rates estimated from sparse, deeper biostratigraphic datums (Teske et al., 2021a; Teske et al., 2021b) and sample availability. On average, 5 g of sediment were taken for each sample. Chronology was based on ^{14}C-AMS analyses (Table 2) performed on 28 bulk sediment samples from Hole U1545A (n = 17) and Hole U1549A (n = 11) at the Rafter Radiocarbon Laboratory, GNS Science, National Isotope Center (Lower Hutt, New Zealand). Radiocarbon ages were converted to calendar years with R statistical software version 4.3.0 (R Core Team, 2023) and Bacon library (Blaauw and Christen, 2011), applying Bayesian statistics with the Marine20 calibration curve (Heaton et al., 2020). Corrections for ^{14}C-AMS ages were performed using a reservoir age of 301 ± 50 years (ΔR) (Goodfriend and Flessa, 1997).

2.4 Micropaleontology

We studied siliceous microfossils, radiolarians and silicoflagellates, in Holes U1545A (Sections U1545A-1H-1 to 5H-7, 41 m depth) and U1549A (Sections U1549A-1H-1 to 4H-2, 28 m depth).

Sampling was performed at ~30 cm resolution in cores from Site U1545A (n = 122), and at ~60 cm resolution in cores from

TABLE 2 Radiocarbon ^{14}C dates and calibrated ages for holes U1545A and U1549A.

Site (A)	Lab code	Depth (mbsf)	Material	AMS 14C age (years BP)	Error	Calibrated age (cal years BP)
U1545	NZA 73592	0.62	Bulk sediment	1,320	20	754
	NZA 73603	4.22	Bulk sediment	3,763	23	3,352
	NZA 73605	6.25	Bulk sediment	5,525	25	5,427
	NZA 73606	7.12	Bulk sediment	6,503	27	6,416
	NZA 73607	8.56	Bulk sediment	7,972	30	7,909
	NZA 73608	13.48	Bulk sediment	11,364	41	12,355
	NZA 73609	13.76	Bulk sediment	11,500	42	12,567
	NZA 73610	14.40	Bulk sediment	12,132	44	13,046
	NZA 73611	14.99	Bulk sediment	12,371	46	13,383
	NZA 73593	15.86	Bulk sediment	12,559	47	13,884
	NZA 76034	20.80	Bulk sediment	15,873	74	18,021
	NZA 73594	25.75	Bulk sediment	19,934	107	22,239
	NZA 73595	29.53	Bulk sediment	21,748	133	24,593
	NZA 73596	30.11	Bulk sediment	22,064	137	24,921
	NZA 73597	34.74	Bulk sediment	24,022	175	27,246
	NZA 73598	40.76	Bulk sediment	28,077	283	30,561
	NZA 73599	42.19	Bulk sediment	28,238	292	31,272
U1549	NZA 73600	1.80	Bulk sediment	1787	21	958
	NZA 73601	3.60	Bulk sediment	2,753	22	1995
	NZA 73602	5.40	Bulk sediment	3,800	24	3,250
	NZA 73604	6.59	Bulk sediment	4,632	25	4,176
	NZA 73752	10.64	Bulk sediment	6,718	28	6,778
	NZA 73753	11.22	Bulk sediment	7,172	28	7,254
	NZA 73754	12.37	Bulk sediment	8,631	32	8,600
	NZA 73756	22.07	Bulk sediment	11,710	43	10,993
	NZA 73757	23.25	Bulk sediment	12,588	47	13,612
	NZA 73758	26.34	Bulk sediment	14,427	56	15,842
	NZA 73759	28.04	Bulk sediment	14,876	59	16,752

NZA: New Zealand (AMS), rafter radiocarbon laboratory.

Hole U1549A (n = 36), at the Gulf Coast Repository of IODP at Texas A&M University, College Station, Texas, United States. Samples were processed in the Laboratorio de Paleoceanografía y Paleoclimas, Instituto de Geofísica, National Autonomous University of Mexico, following the method by Pérez-Cruz (2006). Sediment samples were freeze-dried; 2 g of dry sediment was taken and placed in a beaker with 200 mL of water; later, 20 mL of 35% hydrochloric acid (HCl) and 25 mL of 35% hydrogen peroxide (H_2O_2) were added to dissolve the carbonate components and eliminate the organic matter, and then samples were heated on a rack at ~300°C for 2 hours. Subsequently, the sediments were washed through 37 μm and 25 μm sieves. From the sieve material, slides for petrographic examination were prepared using Entellan mounting medium (refractive index 1.40–1.50 at 20°C). Radiolarians were identified from the >37 μm size fraction and silicoflagellates from the >25 μm size fraction, using a Zeiss light microscope with Planapo objectives (×10, ×20, and ×40). More than 300 specimens of each group of microfossils were identified in each sample to have statistically representative populations (Fatela and Taborda, 2000).

2.5 Statistical analysis

The specimen counts were converted to relative proportions and expressed as percentages of the radiolarian and silicoflagellate populations. A presence/persistence filter was applied to the radiolarian database to highlight the most representative species (more than 1% in the sample). These taxa were considered for applying a Q-mode factor analysis. Factor analysis is a statistical approach used to identify relationships between variables in a large data set (Pisias et al., 2013; Matul et al., 2018) and to resolve these variables into smaller dimensions with minimum loss of information called factors (Hirama et al., 2010). Q-mode factor analysis is one of the standard statistical techniques for estimating the (paleo) environmental parameters from the micropaleontological data archived in marine sediments (MARGO Project Members, 2009; Ortiz, 2011; Matul and Mohan, 2017), and it is used for improving paleoceanographic inferences based on marine micropaleontological quantitative data sets (Loubere and Qian, 1997; Pisias et al., 2013; Matul and Mohan, 2017). In this study, Q-mode factor analysis was performed using R Statistical software version 4.3.0 (R Core Team, 2023), with a maximized variance (VARIMAX) rotation that includes the rotation of the coordinates of data that results from a principal components analysis for maximizing the variance shared among variables. The number of significant factors within the model is usually determined through mathematical criteria by considering the eigenvalues (Molina-Cruz et al., 1999; Pérez-Cruz, 2006). Factor loadings represent the weighting of the factor on any given sample, and Factor scores identify the most relevant species defining the factors. The analysis groups the samples according to their similarity and defines species assemblages that are orthogonal over all samples (Welling et al., 1996).

3 Results

3.1 Chronological frame and sedimentation rates

Radiocarbon dating of the GB sediments provides the chronology frame for our study covering the late Pleistocene (from the late MIS 3) to the Holocene (Table 2; Figures 3A, B). Sedimentation rates were interpolated between calendar-calibrated radiocarbon dates. The time frame for Hole U1545A spans from ~31,260 to 486 cal years BP, and the sedimentation rates ranged from 0.82 mm/yr (~6,416 and 5,427 cal years BP) to 2.48 mm/year (~31,260 and 30,561 cal years BP) (Figure 3A). In Hole U1549A, the time frame spans from ~16,754 to 133 cal years BP, and the sedimentation rates range from 0.41 mm/yr (~8,600 and 7,254 cal years BP) to 1.90 mm/year (16,754 and 15,842 cal years BP) (Figure 3B). The sedimentation rates estimated based on our age models agree with earlier works in the GB. For the end of MIS 3, the estimated rate is 2.48 mm/yr, according to Pichevin et al. (2012), who indicated ~2.2 mm/yr. In our records, the sedimentation rates in the B/A are close to ~2 mm/yr in both holes, in agreement with the 2 mm/yr rate described by Barron et al. (2004). In Hole U1545A during the YD, the sedimentation rate decreased by ~0.25 mm/yr and 1.0 mm/yr in Hole U1549A, similar to the rate suggested by Barron et al. (2004) of the 0.92 mm/yr.

The sedimentation rates from the Holocene in our cores ranged from ~0.82 mm/yr and 0.41 mm/yr, which agree with Barron et al. (2005), who reported 0.88 mm/yr for the past 10,000 years, and with Teske et al. (2019) which estimated rates from 0.23 mm/yr to 1 mm/yr for the last ~5,000 years.

3.2 Radiolarian assemblages

Radiolarians occur throughout the sediment succession in both holes; they are abundant, diverse, and well-preserved. In the samples of the Hole U1545A, 145 radiolarian taxa were found, and 115 taxa in Hole U1549A. The most characteristic taxa ranked by the presence/persistence filter were 26 and 34 in each hole. The Q-mode factor analysis identified four factors explaining more than 80% (U1545A) and 70% (U1549A) of the total variance within the radiolarian data (Table 3). Factor scores denote the importance of the species in each assemblage and are plotted to illustrate which species are grouped together according to the Q-mode analysis (Figures 4, 5). Based on the radiolarian assemblages and their environmental affinities to modern oceanographic conditions (mostly water masses) (see Table 4) in the GB, the factors are termed: 1) *Gulf of California Water,* 2) *Tropical Surface Water,* 3) *Pacific Intermediate Water* and, 4) *California Current Water.* Related to the specific effects of the oxygen concentrations in radiolarians we cannot provide evidence about them; more studies are required with living radiolarians comparing populations dwelling in anoxic and suboxic conditions. Factors loadings were plotted through the time and the main changes are described as follows.

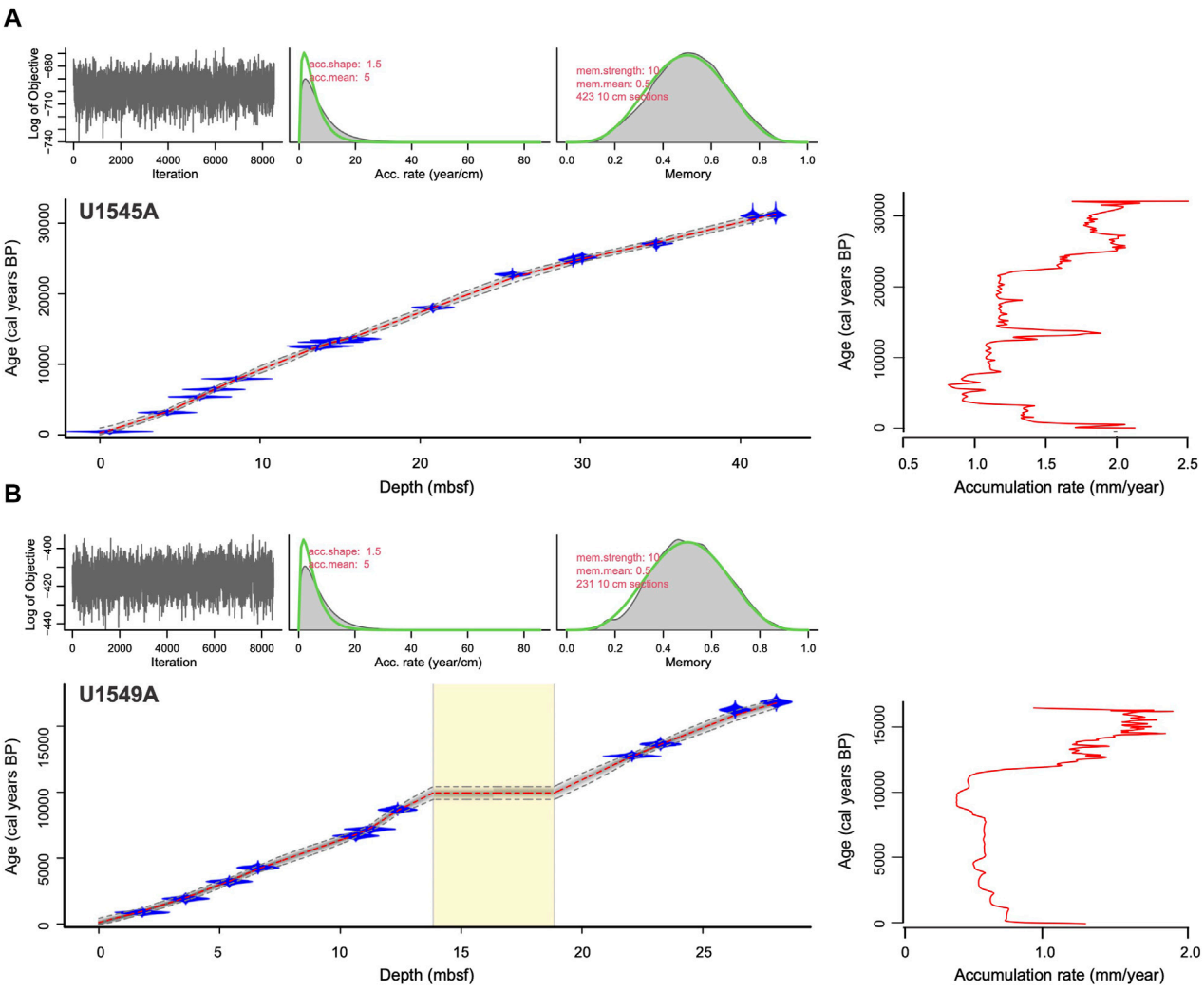

FIGURE 3
Bacon age-depth model for holes **(A)** U1545A and **(B)** U1549A. In each plot, there are indicated Markov Chain MonteCarlo iterations (top left), the distribution of accumulation rates (top middle), and the probability distributions for memory (top right). The lower plot indicates the age-depth model. Individual radiocarbon dates are shown in probability density functions of calibrated ages. The grey area indicates the uncertainty of the age model with dashed lines indicating 95% confidence intervals. On the right side of each plot, sediment accumulation rates are plotted versus age.

TABLE 3 Eigenvalues from Q-mode Factor Analysis, showing the importance of the four radiolarian assemblages (factors).

Site (A)	Factor	Factor name	Eigenvalue	Accumulated eigenvalues	Total variance (%)	Accumulated variance (%)
U1545	1	PIW	51.31	51.31	42	42
	2	TSW	26.18	77.49	22	64
	3	CCW	11.63	89.13	10	74
	4	GCW	7.25	96.38	6	**80**
U1549	1	TSW	13.83	13.83	48	48
	2	PIW	3.02	16.86	10	58
	3	GCW	1.86	18.72	7	65
	4	CCW	1.50	20.23	5	**70**

Bold values depict the total variance explained with four factors in each site.

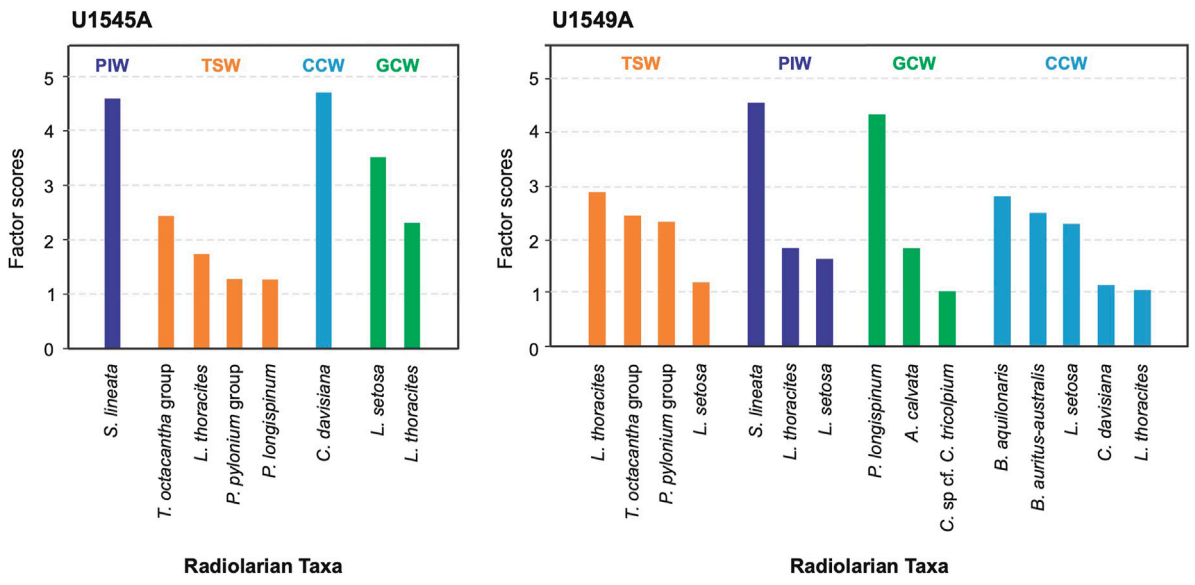

FIGURE 4
Factor scores of the radiolarian taxa characterizing the four radiolarian assemblages in holes U1545A and U1549A.

3.2.1 Hole U1545A

Factor 1, termed *Pacific Intermediate Water*, explains 42% of the total variance (Table 3). It shows its highest values, with slight fluctuations in four intervals from ~30,690 to 24,755, 19,770 to 18,790, 18,050 to 14,360, and 13,400 to 12,200 cal years BP (Figure 6B). The lowest values of the factor occur throughout the Holocene; it is represented by *Siphocampe lineata* with a factor score of 4.59 (Figure 4). This species is a dweller of cold waters and ocean fronts (Boltovskoy and Riedel, 1987), inhabiting water depths from 300 to 1,000 m in the northern Pacific Ocean (Kling and Boltovskoy, 1995). Its highest abundances are restricted to high latitudes (Boltovskoy and Correa, 2016) in the arctic and subarctic regions of the northern Pacific Ocean (Takahashi, 1991; Kling and Boltovskoy, 1995; Boltovskoy and Correa, 2016). It was previously associated with the PIW in the GoC (Bernal-Ramírez, 2003). Thus, its dominant occurrence in this factor suggests the PIW flow strengthened in Hole U1545A during these intervals.

Factor 2, termed *Tropical Surface Water*, explains 22% of the total variance (Table 3). It shows its highest values in the Holocene from ~11,300 to 640 cal years BP, in episodic intervals from ~30,980 to 30,390, 28,340 to 27,400, and 14,110 to 12,090 cal years BP, and depicts peaks at ~24,750, 19,030, and 15,350 cal years BP (Figures 6A, B). This factor is represented by *T. octacantha* group, *L. thoracites, Phorticium pylonium* group, and *Peridium longispinum,* with factor scores of 2.43, 1.75, 1.29, and 1.29, respectively (Figure 4). Members of the *T. octacantha* group are surface dwellers distributed mainly at 0–75 m depth in productive areas where chlorophyll-*a* is high (Ishitani and Takahashi, 2007; Hu et al., 2015), and it is an indicator of the tropical thermocline (Hu et al., 2015). This taxonomic group has been identified as the leading radiolarian species from the central equatorial Pacific (Welling et al., 1996). In the GoC, it was previously reported in the Pescadero and Farallon basins, coherent with the occurrence of the inflow of warm water mass in the southern gulf (Fernández-Barajas et al., 1994; Molina-Cruz et al., 1999). *L. thoracites* dwells in surface waters, from 0 to 100 m depth (Abelmann and Gowing, 1997), and it is the predominant species in the water surface of the GB (Molina-Cruz et al., 1999) and was associated with the TSW (Pisias, 1986), and with highly productive waters (Pisias, 1986). It is important to mention that, in the past, it was considered a group rather than a single species and was found to be a significant component of an assemblage related to winter conditions on the Pacific coast (Welling and Pisias, 1993). Members of *P. pylonium* group have a cosmopolitan distribution and they dwell in the upper 150 m of the water column in the ETPO (Boltovskoy et al., 2010). The group has been linked to upwelling along the western GoC and to strengthened SE winds (Molina-Cruz et al., 1999). *P. longispinum* is a surface mixed-layer dweller from 100 to 150 m depth in the GoC (Molina-Cruz et al., 1999) growing in similar environmental conditions of temperature and salinity to those described for *L. thoracites*, and in highly oxygenated waters, from 5 to 7 mL/L in the Pacific Ocean (Tanaka and Takahashi, 2008). Thus, the environmental affinities of this radiolarian assemblage suggest the inflow of the TSW in the GB, as seen nowadays by the weakening of NW winds and the strengthening of SE winds (Marinone, 2003; Amador et al., 2006). Furthermore, the occurrence of *L. thoracites*, *P. pylonium* group, and *P. longispinum*, may indicate the development of local upwelling processes on the western margin of the GoC, or the advection of nutrient-rich waters, mainly due to coastally-trapped waves in summer, internal waves, and/or the influence of cyclonic gyres.

Factor 3, termed *California Current Water*, explains 10% of the total variance (Table 3). It shows the highest importance during the late Pleistocene, from ~30,830 to 28,670, 27,400 to 21,490, and 13,710 to 13,210 cal years BP, and in a peak at ~11,820 cal years BP (Figure 6B). *Cycladophora davisiana* represents this factor with a factor score of 4.70 (Figure 4). This species dwells in intermediate-depth water ranging from ~200 to 500 m depth in Southern

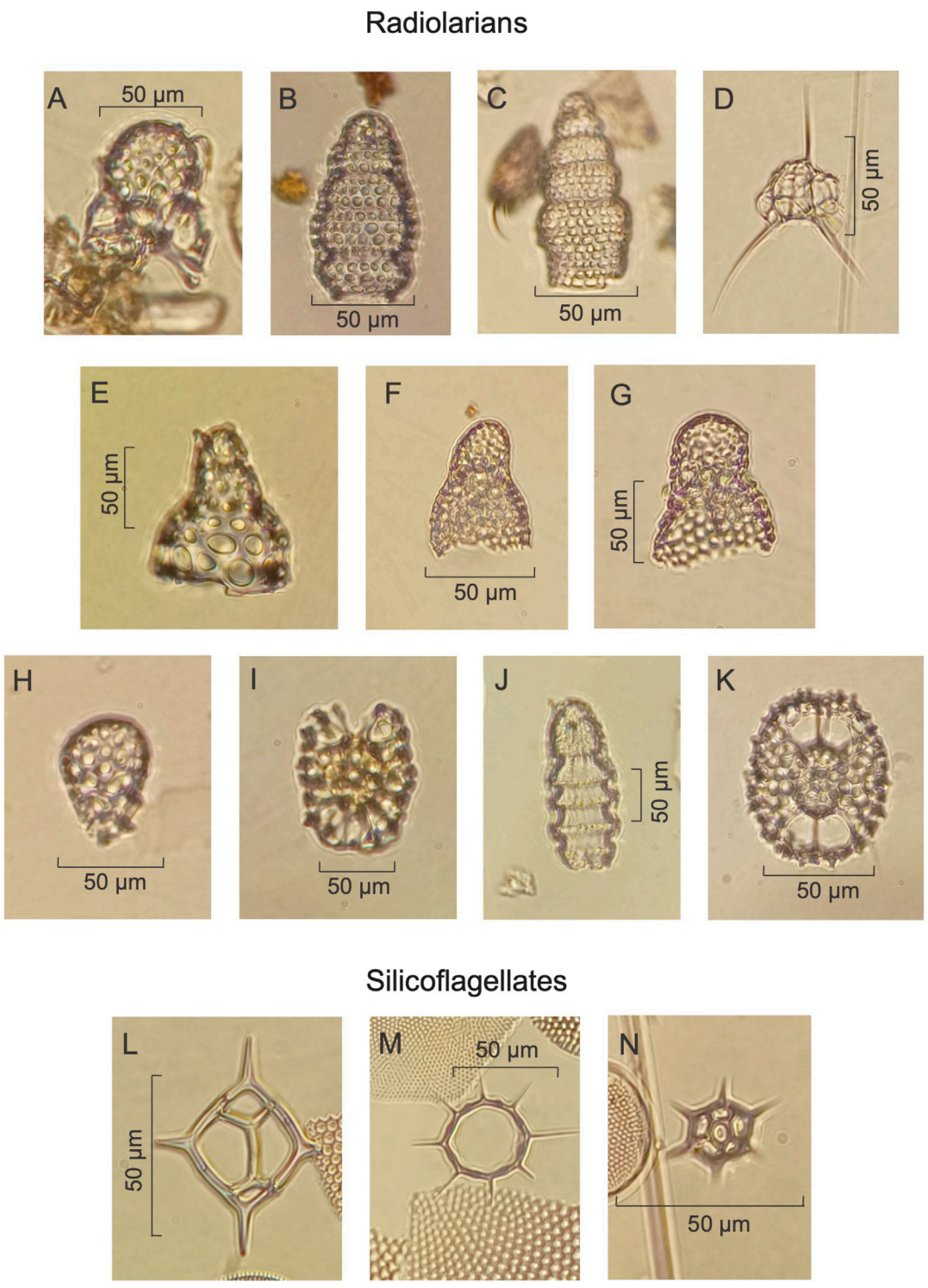

FIGURE 5
Siliceous microfossils. Radiolarians **(A)** *Arachnocorallium calvata*, **(B)** *Botryostrobus aquilonaris*, **(C)** *B. auritus-australis*, **(D)** *Cladoscenium* sp cf. *C. tricolpium*, **(E)** *Cycladophora davisiana*, **(F)** *Lithomelissa setosa*, **(G)** *L. thoracites*, **(H)** *Peridium longispinum*, **(I)** *Phorticium pylonium* group, **(J)** *Siphocampe lineata*, **(K)** *Tetrapyle octacantha* group. Silicoflagellates **(L)** *Dictyocha fibula* var. *messanensis*, **(M)** *Octactis octonaria* var. *pulchra*, **(N)** *Octactis speculum*.

California Current and the Okhotsk Sea (Kling and Boltovskoy, 1995; Nimmergut and Abelmann, 2002; Okazaki et al., 2003), and at subsurface waters in the Eastern Pacific, from 50 to 150 m depth (Boltovskoy et al., 2010). It was associated with the thermohaline fronts at the mouth of the GoC and with the CCW (Molina-Cruz, 1986). *C. davisiana* showed significantly high values in the glacial periods (e.g., Morley, 1980), indicating that it can serve as a proxy for glacial conditions. The presence of this species during the late

TABLE 4 Environmental affinities of the radiolarians and silicoflagellates used in this study to reconstruct the oceanographic changes in the Guaymas Basin.

Taxa	Samples	Environmental affinities	Related water mass	References
Radiolarians				
Arachnocorallium calvata Petrushevskaya, (1971)	Surface sediments	Surface dweller (upper 100 m depth); associated with mixing processes and the GCW in the GB.	GCW	Molina-Cruz et al. (1999)
Botryostrobus aquilonaris Bailey, (1856)	Column water and surface sediments	Inhabits the CCW and is related to oceanic fronts in the GoC. It is associated with C. davisiana and B. auritus-australis	CCW	Benson, (1966); Molina-Cruz, (1986); Kling and Boltovskoy, (1995)
Botryostrobus auritus-australis Nigrini, (1977)	Column water and surface sediments	Surface dweller (0–150 m depth), it is related to the CCW.	CCW	Boltovskoy and Riedel, (1987); Kling, (1979)
Cladoscenium sp cf. C. tricolpium Benson, (1966)	Column water	Surface dweller (40–200 m depth), related to upwelling regions enriched in nitrates and silicates	GCW	Yamashita et al. (2002)
Cycladophora davisiana Ehrenberg, (1862)	Column water and surface sediments	Inhabits from 50 to 150 m depth in the Eastern Pacific. It is associated with thermohaline fronts in the GoC, related to CCW, and it is an indicator of glacial conditions	CCW	Morley, (1980); Molina-Cruz, (1986); Kling and Boltovskoy, (1995); Boltovskoy et al., 2010
Lithomelissa setosa Jorgensen, (1900)	Column water and surface sediments	Surface dweller (0–120 m depth); inhabits above the mixed layer. It is an indicator of upwelling and boreal spring conditions in the northern Pacific	GCW	Takahashi, (1987); Ishitani and Takahashi, (2007); Lüer et al. (2008)
Lithomelissa thoracites Haeckel, (1862)	Column water and surface sediments	Inhabits the upper 100 m depth. It is a predominant species in the surface waters of the GB and it is associated with highly productive waters	GCW	Pisias, (1986); Welling and Pisias, (1993); Molina-Cruz et al. (1999)
Peridium longispinum Jorgensen, (1900)	Column water and surface sediments	Surface mixed-layer dweller (100–150 m depth) in the GoC. It is associated with productive waters	GCW	Molina-Cruz et al. (1999); Tanaka and Takahashi, (2008)
Phorticium pylonium group Haeckel, (1887)	Column water and surface sediments	Surface dweller (upper 150 m depth in the ETPO). It is associated with upwelling along the western GoC and strengthened SE winds	TSW	Takahashi, (1991); Molina-Cruz et al. (1999); Boltovskoy et al. (2010)
Siphocampe lineata Ehrenberg, (1838)	Column water and surface sediments	Intermediate dweller (300–1,000 m depth) in the North Pacific. It has been related to the PIW in the GoC	PIW	Bernal-Ramírez, (2003); Boltovskoy and Correa, (2016)
Tetrapyle octacantha group Müller, (1858)	Column water and surface sediments	Inhabits from 0 to 75 m depth, it is an indicator of the tropical thermocline. In the GoC, it is related to tropical waters	TSW	Welling et al. (1996); Hu et al. (2015)
Silicoflagellates				
Dictyocha fibula var. messanensis Lemmerman, (1901)	Column water and surface sediments	It is related to oligotrophic tropical waters and high SST values	TSW	Pérez-Cruz and Molina-Cruz, (1988); Onodera and Takahashi, (2005)
Octactis octonaria var. pulchra Guiry and Guiry, (2023)	Column water and surface sediments	Inhabits cold surface waters (15°C–23 °C) in highly productive regions indicating upwelling and mixing processes	GCW	Schrader and Murray, (1985); Schrader et al. (1986)
Octactis speculum Chang et al. (2017)	Column water and surface sediments	Inhabits relatively cold waters. In the GoC, it has been associated with the incursion of the CCW.	CCW	Murray and Schrader, (1983); Barron et al. (2014)

Pleistocene, mainly during the LGM, ~26,500 and 22,000 cal years BP, suggests the incursion of the CCW into the gulf, reaching the GB (~27°N), during extreme-cold conditions when the ice volume increased globally, and the polar atmospheric cell expanded (Figures 7A, C, 8E). This setting amplified its influence southward modifying the position of the polar and subtropical atmospheric jets and displacing the CCS that enabled the entry of CCW into the gulf.

Factor 4, termed *Gulf of California Water*, explains 6% of the total variance of data (Table 3). The highest values of this factor are from ~31,120 to 24,750, 21,730 to 17,060, and from 7,620 to 490 cal years BP; and some episodic peaks are identified at ~14,110, 13,210, and 9,990 cal years BP (Figure 6B). This factor is composed of *L. setosa* and *L. thoracites*, with factor scores of 3.52 and 2.31, respectively (Figure 4). *L. setosa* dwells in the upper 120 m of the water column (Kling and Boltovskoy, 1995; Yamashita et al., 2002; Ishitani and Takahashi, 2007; Tanaka and Takahashi, 2008) above the mixed layer and the thermocline (Yamashita et al., 2002; Lüer et al., 2008), in oxygenated water masses (5–7 mL/L) with a salinity of 34–35.5 g kg^{-1} (Yamashita et al., 2002; Tanaka and Takahashi, 2008), serving as an indicator of upwelling processes (Ishitani and Takahashi, 2007). *L. setosa* has been associated with interglacial periods as a marker of boreal spring conditions in the northern Pacific Ocean (Takahashi, 1987). The environmental affinities of *L. thoracites* have been previously described

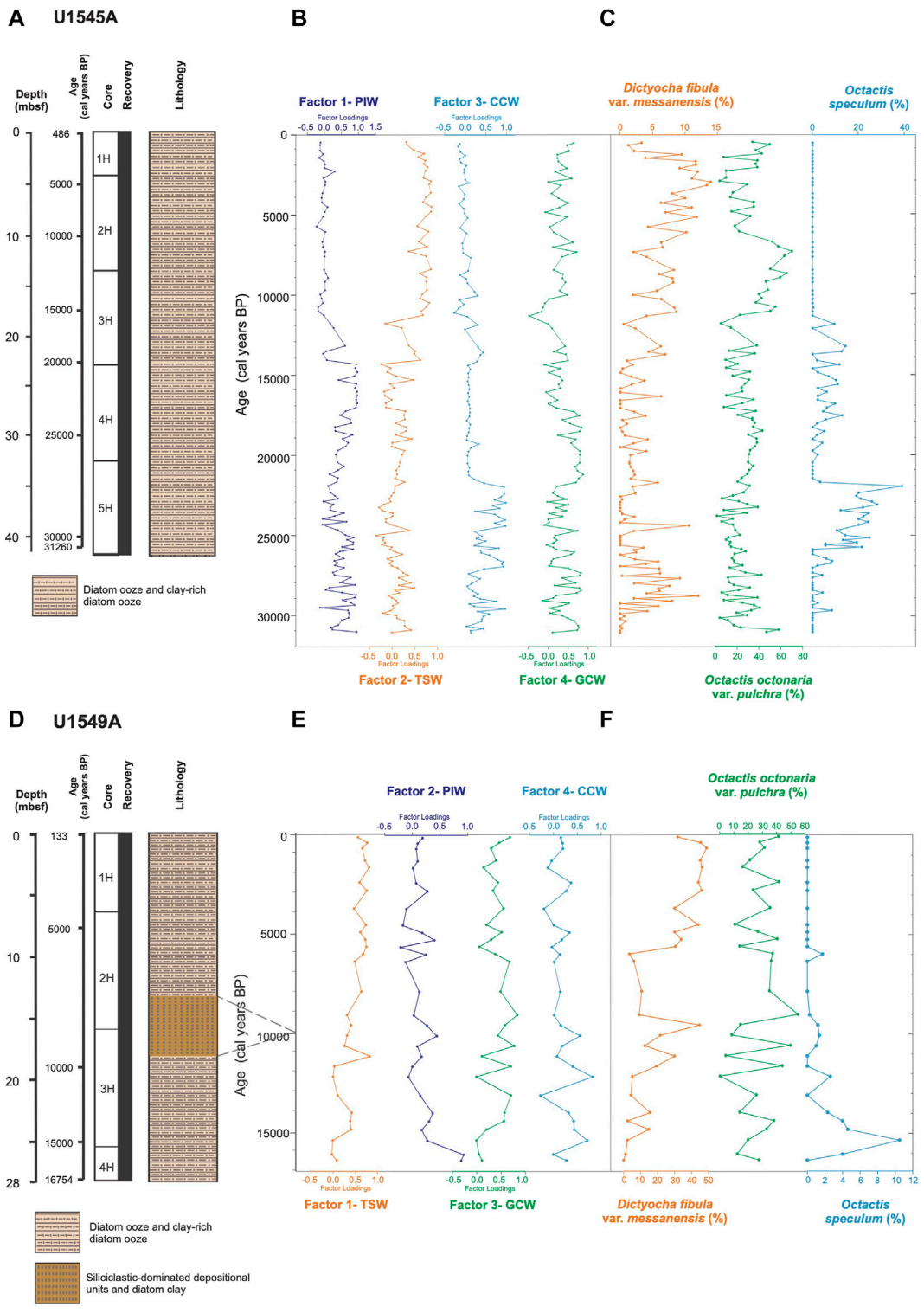

FIGURE 6
(A) Stratigraphic column of the Hole U1545A showing lithology (Teske et al., 2021b). **(B)** Factor loadings of the four factors identified from the Q-mode factor analysis and **(C)** relative abundances of silicoflagellates in Hole U1545A. **(D)** Stratigraphic column of the Hole U1549A showing lithology (Teske et al., 2021a). **(E)** Factor loadings of the four factors identified from the Q-mode factor analysis and, **(F)** relative abundances of silicoflagellates in Hole U1549A.

for Hole U1545A. Hence, the assemblage suggests the occurrence of the GCW-like water mass in the basin. These conditions could be similar to the current cold winter-spring phase in the gulf, when the NW winds are strengthened, due to the southward NPH migration, promoting the intensification of upwellings and mesoscale gyres, and the increase of productivity.

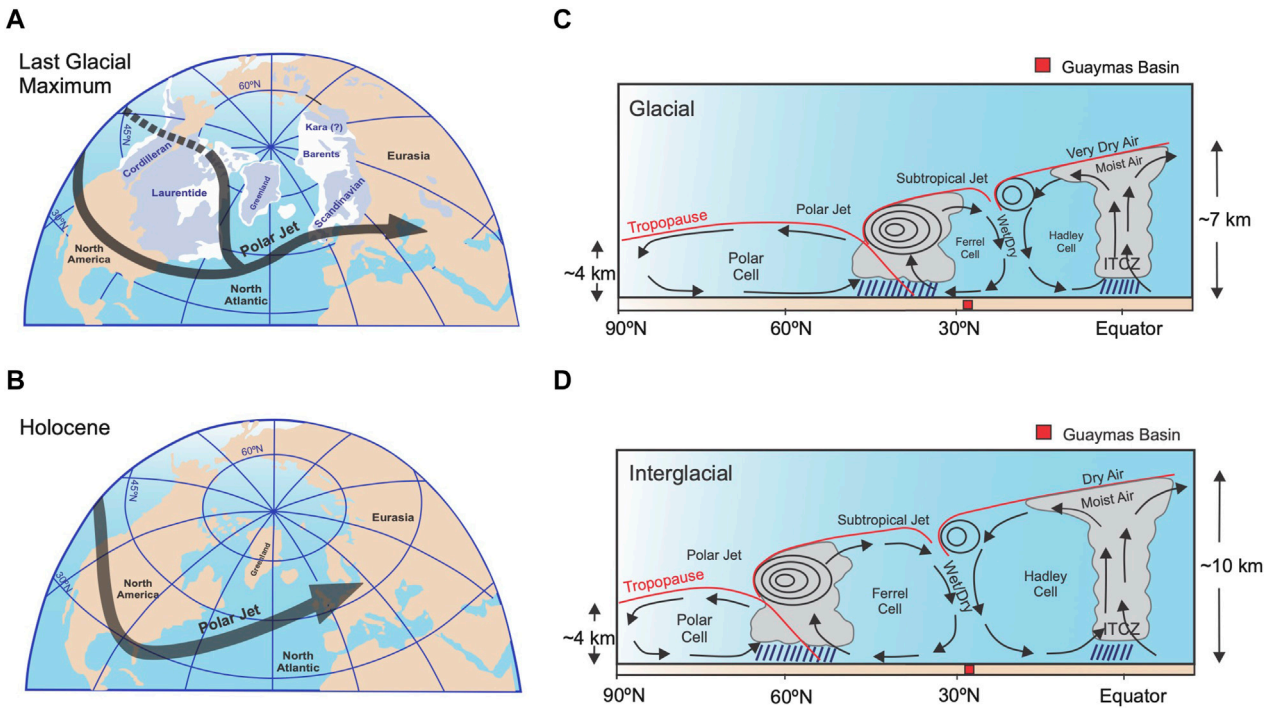

FIGURE 7
Polar jet stream position (black arrow) during **(A)** the Last Glacial Maximum and, **(B)** the Holocene (Hughes et al., 2013). Climate cell boundaries in the northern hemisphere during **(C)** the Last Glacial Maximum and **(D)** the Holocene (Cheshire and Thurow, 2013). Guaymas basin is positioned at 27°N (red square).

3.2.2 Hole U1549A

Factor 1, termed *Tropical Surface Water*, explains 48% of the total variance (Table 3), and showed its highest values from ~11,500 to 11,000 and from 8,700 to 133 cal years BP (Figures 6D, E). This factor is represented by the species *L. thoracites*, by the *T. octacantha* group, the *P. pylonium* group, and by *L. setosa*. Factor scores of these species are 2.87, 2.45, 2.32, and 1.20, respectively (Figure 4). In Hole U1549A, this radiolarian assemblage indicates of TSW into the basin, suggesting the strengthened SE winds. *L. thoracites* in this assemblage indicates the occurrence of the GCW in the location of drilling.

Factor 2, termed *Pacific Intermediate Water*, represents 10% of the total variance (Table 3). The highest values of this factor are from ~16,450 to 13,170, 10,600 to 9,600, 5,400 to 4,930, and from 2,840 to 2,620 cal years BP (Figure 6E). The species representing this factor are *S. lineata*, *L. thoracites,* and *L. setosa*, with factor scores of 4.57, 1.82, and 1.62, respectively (Figure 4). Environmental affinities of these species were previously described (Takahashi, 1987; Tanaka and Takahashi, 2008) and suggest (mainly in *S. lineata*) increased incursion of the PIW into the GB; besides, *L. thoracites* and *L. setosa* indicate the occurrence of the GCW.

Factor 3, termed *Gulf of California Water*, explains 7% of the total variance (Table 3). It shows its highest values from ~14,500 to 12,800, 12,000 to 11,520, 10,900 to 6,040, 5,100 to 4,710, 4,150 to 3,020, and from 480 to 130 cal years BP (Figure 6E). This factor is represented by *P. longispinum*, *Arachnocorallium calvata,* and *Cladoscenium* sp cf. *C. tricolpium*. Factor scores of these species are 4.34, 1.84, and 1.02, respectively (Figure 4). The environmental affinities of *P. longispinum* have been previously described (Molina-Cruz et al., 1999). *A. calvata* is a surface dweller in the upper 100 m depth; being a species that is part of the radiolarian assemblage related to mixing processes and the GCW in the GB (Molina-Cruz et al., 1999). *C.* sp cf. *C. tricolpium* is a surface dweller from 40 to 200 m depth in upwelling regions enriched in nitrates and silicates (Yamashita et al., 2002). Thus, the radiolarian assemblage suggests the occurrence of the GCW in similar conditions as those currently occurring during the winter-spring phase in the GoC.

Factor 4, termed *California Current Water*, explains 5% of the total variance (Table 3). The highest values are from ~16,010 to 13,900, 12,520 to 11,410, 10,670 to 9,630, 5,310 to 4,730, and from 3,020 to 2,250 cal years BP (Figure 6E). This factor is represented by *B. aquilonaris*, *L. setosa*, *B. auritus-australis*, *C. davisiana* and *L. thoracites,* with factor scores of 2.82, 2.49, 2.30, 1.14 and 1.07, respectively (Figure 4). *B. aquilonaris* inhabits the CCW (Kling and Boltovskoy, 1995), with its occurrence related to oceanic fronts formed by the encounter of CCW and the TSW in the mouth of the gulf (Molina-Cruz, 1986). This species is associated with *C. davisiana* and *B. auritus-australis* (Benson, 1966). *B. auritus-australis* is a surface dweller from 0 to 150 m depth (Kling, 1979; Boltovskoy and Riedel, 1987; Tanaka and Takahashi, 2008) and is related to the CCW (Benson, 1966; Kling, 1979; Molina-Cruz, 1986). It is less abundant in the present-day GoC waters compared to the last glacial period (Molina-Cruz, 1986). The presence of *B. aquilonaris, B. auritus-australis,* and *C. davisiana* in this factor suggests the incursion of CCW into the GB during extreme-cold

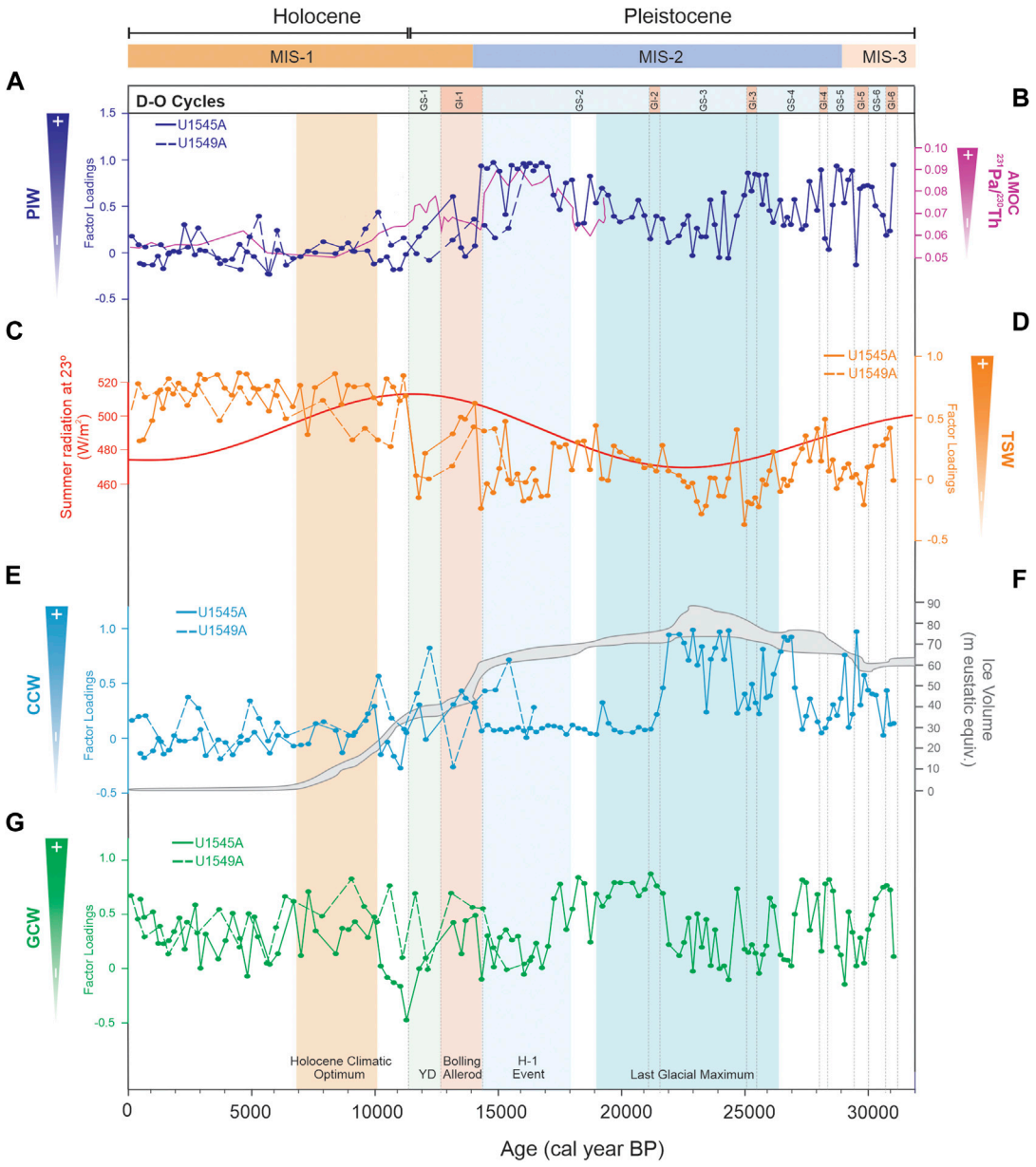

FIGURE 8
(A) Factor loadings of Pacific Intermediate Water radiolarian assemblage in holes U145A (continuous line) and U1549A (dashed line); **(B)** Sedimentary $^{231}Pa/^{230}Th$ ratio record (McManus et al., 2004); **(C)** Incoming solar radiation on Earth´s surface during summer at 23°N (W/m^2) (Berger and Loutre, 1991); **(D)** Factor loadings of the Tropical Surface Water radiolarian assemblage in holes U145A (continuous line) and U1549A (dashed line); **(E)** Factor loadings of the California Current Water assemblage in holes U1545A (continuous line) and U1549A (dashed line); **(F)** Ice volume of the Laurentide ice sheet during the last glacial cycle. Ice volume values are eustatic equivalent metres of sea level (Hughes et al., 2013); **(G)** Factor loadings of the Gulf of California Water assemblage in holes U1545A (continuous line) and U1549A (dashed line).

conditions when the polar atmospheric cell expanded and amplified its influence southward.

3.3 Silicoflagellates

Silicoflagellates are abundant and well-preserved in sediments from both holes, with 16 species identified in Hole U1545A and 15 species in Hole U1549A. Based on their environmental affinities three species can be used as SST and water masses proxies: *Octactis octonaria* var. *pulchra*, *O. speculum, and Dictyocha fibula* var. *messanensis* (See Table 4; Figure 5).

3.3.1 Hole U1545A

O. octonaria var. *pulchra* shows an abundance of 1.5%–70.2%, averaging at 27.3%. Its highest values are from ~29,770 to 27,560, 21,240 to 18,060, 11,300 to 6,080, and from 2070 to 490 cal years BP (Figure 6C). This species is related to cold surface waters (15°C–23 °C) in highly productive and upwelling regions (Schrader et al., 1986). In the GoC, during summer-fall, it is distributed in the

northern GoC, in contrast to winter-spring, when it is found from the region mouth to 27°N, i.e., at GB latitude (Murray and Schrader, 1983; Schrader et al., 1986). This species is characteristic of the GB, where the upwelling and mixing processes are enhanced by tidal dynamics (Schrader and Murray, 1985). According to its environmental affinities, the presence of this species suggests the dominance of the GCW in the basin and climatic conditions similar to the ones currently occurring during winter-spring in the GoC, characterized by the strengthening of NW winds, and the development of wind-driven upwelling and mesoscale gyres and productivity (Douglas et al., 2007).

The relative abundance of *O. speculum* ranged from 0% to 38.9%, with an average of 4.9%. The highest abundance of this species is observed from 25,800 to 21,730 cal years BP and from 17,800 to 11,820 cal years BP (Figure 6C). This species inhabits relatively cold waters, restricted by the 10°C–22°C isotherms (Murray and Schrader, 1983). In the GoC, it has been associated with the incursion of the CCW (Barron et al., 2014). This species is more abundant in the mouth region, but in late Pleistocene sediments, it has also been found in mid-latitudes (27°N) (Barron et al., 2014). Thus, the climatic scenario proposed for these intervals is inferred as the result of an incursion of the CCW into the GB due to the expansion under the influence of the polar cell and the southward migration of the CCS.

D. fibula var. *messanensis* shows an abundance of 0%–15.6%, and an average of 3.8%. The highest abundances are registered from ~29,770 to 26,670, 13,900 to 12,510, and from 11,290 to 990 cal years BP (Figure 6C). Some peaks are recognized at ~24,410, 21,730, and 16,330 cal years BP. In the GoC, this species is related to warm surface waters (18°C–26°C), such as the TSW (Schrader et al., 1986) and to the increase of SST in the Pacific Ocean (Onodera and Takahashi, 2005). This species is considered an indicator of oligotrophic conditions (Takahashi, 1991). It has been found in the mouth region and during ENSO events, reaching as far north as 26 to 28°N (Pérez-Cruz and Molina-Cruz, 1988). The presence of this species in the sediments suggested a greater incursion of the TSW into the gulf, enhanced by the weakening of NW winds and the strengthening of SE winds, as occurs during the current boreal summer.

3.3.2 Hole U1549A

The abundance of *O. octonaria* var. *pulchra* ranges from 0.3% to 55%, and the average was 27.1%. The highest values of this species were recorded from ~9,300 to 5,910 cal years BP. Other minor intervals were recognized from ~15,010 to 14,230, 11,820 to 11,460, 10,920 to 10,390, 5,420 to 4,930, 4,010 to 3,020, 2,630 to 1960, and from 900 to 130 cal years BP (Figure 6F). Its presence in the sediments suggests the above-mentioned environmental conditions in Hole U1545A.

D. fibula var. *messanensis* shows an abundance ranging from 0% to 48.8%. The average relative abundance is 23.4%. This species shows three intervals of higher abundance, from ~11,610 to 11,000, 10,150 to 9,320, and from ~5,740 to 130 cal years BP (Figure 6F). The increase in the abundance of this species is attributed to a more evident incursion of the TSW into the gulf, enhanced by the weakening of NW winds and the strengthening of SE winds.

O. speculum has an abundance ranging of 0%–10.5% and an average of 1.2%. Its presence is almost exclusively restricted to the Pleistocene, which showed its highest values from ~16,450 to 13,810 cal years BP. Other minor intervals were recognized from ~12,620 to 12,010, 10,670 to 9,620 cal years BP, and a peak located at ~6,030 cal years BP (Figure 6F). The presence of this species is probably related to the incursion of the CCW into the gulf, resulting from the polar atmospheric cell expansion and the strengthening of the CCS.

4 Discussion

Our aim is to interpret ocean vertical water masses history and the significant trends in the GB, including changes in deep water masses, our analyses presented some constraints. The signal of StSsW (Table 1) was not evident and might have been masked by the presence of the salty water-related radiolarian assemblage from the GCW resulting from the formation of the StSsW by subduction of salty cold surface waters in the northern GoC during winter (Lavin and Marinone, 2003; Portela et al., 2016), ultimately resulting in the formation of GCW (Lavin and Marinone, 2003). The PDW could not be identified because of the lack of knowledge of the radiolarian living species in deep water environments in GoC and other regions in the Pacific Ocean. However, we consider that the signal of the water masses captured in our records represents the main trends in ocean circulation in the GoC and its relationship with the dynamics of the ETPO and global climate changes.

4.1 Pre—LGM time (~31,260–26,500 cal years BP)

In this interval, the microfossil records suggest mainly the alternation of surface waters similar to the GCW and the CCW (Figure 8E, 8G, 9E). Compared to the Holocene, the occurrence of the PIW in the GB is significant (Figure 8A), because of the glacial conditions and the significantly higher formation of the North Pacific Intermediate Water (NPIW) which expanded further than present-day (Gong et al., 2019). When GCW-like water was present, weather conditions must have been similar to current winter conditions in that area, causing the GCW to form. However, the alternation of GCW and CCW in the GB could be related to the amplification of the polar atmospheric cell (Cheshire and Thurow, 2013), which modified the location of the polar and subtropical jet streams (to 45° and 20°N, respectively; Figure 7C) (e.g., Andrews and Dyke, 2007; Cheshire and Thurow, 2013). Consequently, the southward migration of the CCS and the CCW (McClymont et al., 2012) allowed it to reach the tip of the Baja California peninsula (Barron et al., 2014; Molina-Cruz, 1986; Figure 1A) and enhanced its incursion into the gulf, moving to the northern GB. Additionally, in this interval, episodic events are recognized where the incursion of TSW is proposed (Figures 8D, 9B). These events are related to two GIs events (6 and 4) with summer-like conditions. In previous studies, it has been suggested that the location of the NPH was shifted south during the transition from MIS-3 to MIS-2, weakening the NW winds during winter and strengthening them during summer (Cheshire and Thurow, 2013), resulting in summer-like conditions, and warm and

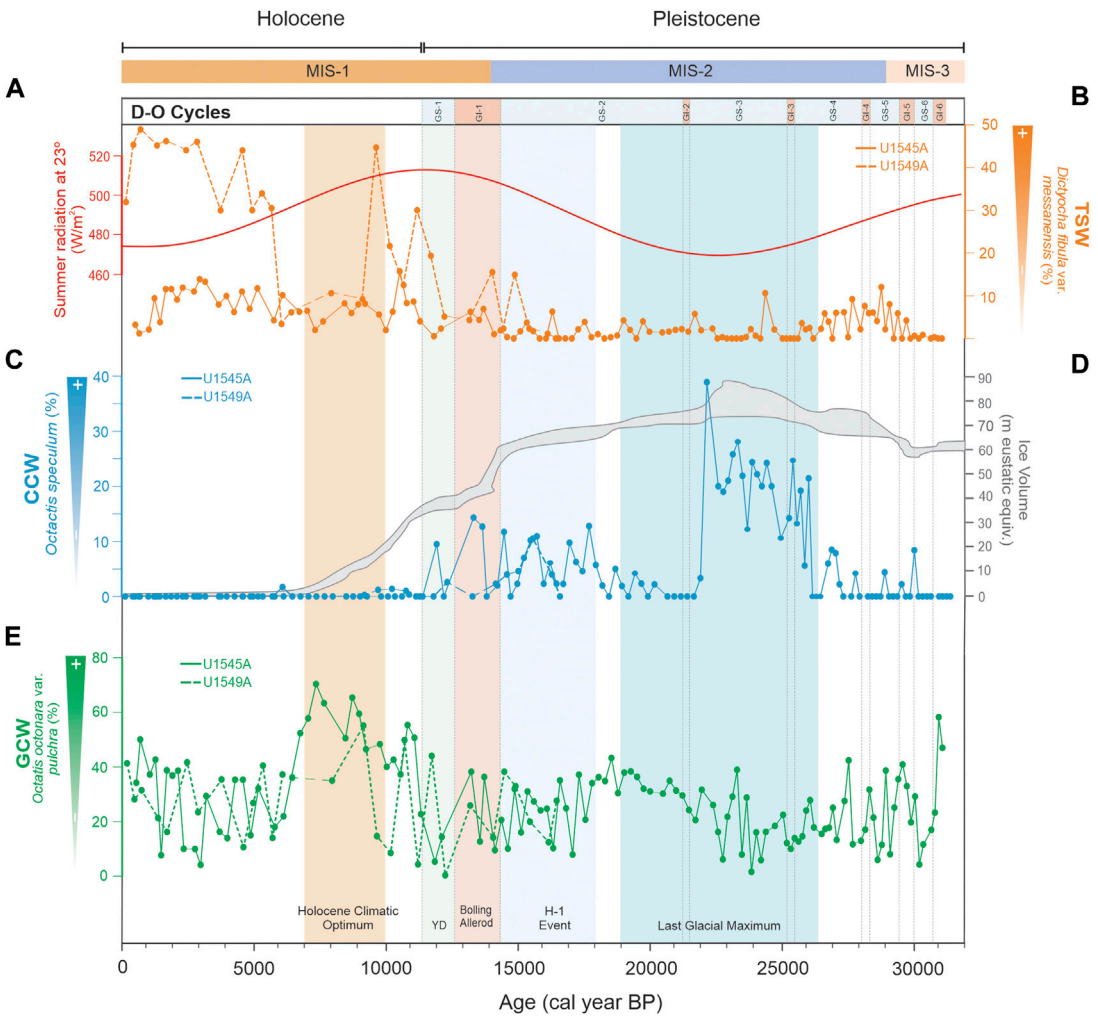

FIGURE 9
(A) Incoming solar radiation on Earth's surface during summer at 23°N (W/m^2) (Berger and Loutre, 1991). **(B)** Relative abundances of *Dictyocha fibula* var. *messanensis* in holes U145A (continuous line) and U1549A (dashed line); **(C)** Relative abundances of *Octactis speculum* in holes U1545A (continuous line) and U1549A (dashed line); **(D)** Ice volume of the Laurentide ice sheet during the last glacial cycle. Ice volume values are eustatic equivalent metres of sea level (Hughes et al., 2013); **(E)** Relative abundances of *Octactis octonaria* var. *pulchra* in holes U1545A (continuous line) and U1549A (dashed line).

stratified conditions during MIS 3 (Barron et al., 2014). This enabled the formation of the laminated sediments, as is observed in our sedimentary records (Supplementary Figure S2). Also, GS events (6, 5, and 4) were identified where the PIW and CCW prevailed (Figure 8A, 8E, 9C) due to the amplification of the polar atmospheric cell (Figure 7A, 7C).

4.2 LGM (~26,500–19,000 cal years BP)

During this interval, two water masses dominated the GB: CCW and PIW (Figure 8A, 8E, 9C). For the time of ~24,750 to 21,490 cal years BP, when the Laurentide ice sheet reached its maximum volume (Figure 7A, 8F, 9D) and the summer insolation in the Northern Hemisphere was low (Barron et al., 2014; Figures 8C, 9A) our data suggest the strengthening of the CCS, causing the incursion of the CCW into the GB, particularly during the GS-4 and GS-3 (Figures 8E, 9C). Our results are in agreement with Barron et al. (2014), who indicated that during MIS2, in comparison to MIS3, cold water with low salinity occurred in the GB, which may suggest the presence of CCW-like during this period. Besides, the less saline water could be related to the increase in precipitation, as Cheshire and Thurow (2013) suggested, due to the latitudinal migration of the NPH and the polar jet stream southward (Figure 7A). Further, our records indicate the significant presence of the PIW at the beginning and the end of the interval (Figure 8A), which might be related to favorable conditions for forming NPIW (Okazaki et al., 2012) and thus its incursion into the GB. In contrast, the dominance of the GCW at the end of the interval (Figures 8G, 9E) in the GI-2 suggests climatic conditions similar to those described for GIs in the pre-LGM. The formation of the PIW was less intense from 23,500 to 21,240 cal years BP (Figure 8A) owing to (1) the advection of subtropical waters to the subarctic Pacific Ocean was constrained, (2) the weakened thermohaline circulation (Pichevin et al., 2012), and (3) the surface-ocean halocline inhibiting the formation of the NPIW (Gong et al., 2019).

4.3 Deglaciation (~19,000–11,700 cal years BP)

This interval, also known as Termination-I, is considered a transition from glacial to interglacial conditions and includes remarkable climatic events such as the Heinrich-1 event, the Bølling-Ållerød (B/A), and Younger Dryas.

4.3.1 Heinrich-I event (~19,000–14,900 cal years BP)

We identify two major climatic conditions in this interval: from ~18,540 to 17,060 and between ~17,060 and 14,350 cal years BP (HE-1). The former revealed GCW-like water dominance in GB (Figures 8G, 9E). At that time, the weakened Atlantic Meridional Overturning Circulation (AMOC) (Figure 8B) (McManus et al., 2004) and the southernmost position of the ITCZ in the Pacific Ocean drove a reduction of precipitation and the establishment of the Pacific Meridional Overturning Circulation (PMOC), which led to the abnormal poleward surface currents transporting more saline subtropical waters into the North Pacific (Gong et al., 2019) and probably into the GoC, causing the flow of GCW-like waters into to GB. Furthermore, from 17,060 to 14,350 cal years BP, our proxy records suggest changes in the surface waters, mainly in the central GB, consistent with the occurrence of the CCW (Figures 8E, 9C). These changes in the water masses structure may be related to a significant reorganization in the North Pacific that occurred during the last glacial termination when a glacial mode transformed into an interglacial mode. This reorganization in the climate system could have caused gradual northward migration of the ITCZ, which caused the weakening of the northwesterly winds, as Price et al. (2012) suggested. Throughout this interval, from ~18,540 to 14,350 cal years BP, the PIW was considerably dominant in the GB at both sites studied (Figure 8A), which is congruent with models that suggest a deep-water formation in the North Pacific extending to a water depth of ~2,500–3,000 m during H1 (Okazaki et al., 2012).

4.3.2 Bølling-Ållerød (~14,900–12,800 cal years BP)

This interval corresponds to GI-1 from 14,491 to 12,711 cal years BP (Björck et al., 1998). In Hole U1545A in the northwestern GB, two types of surface water masses occurred in alternate intervals: (1) the TSW from 14,100 to 13,540 cal years BP, and (2) the CCW from 13,540 to 13,210 cal years BP (Figures 8D, E, 9B, C); the PIW caused a significative peak at 13,210 cal years BP (Figure 8A). In Hole U1549A in the central GB, the alternation of the GCW and TSW dominated at the beginning of the interval, from 14,050 to 13,180 cal years BP (Figures 8D, G, 9B, E), and the PIW had a significant pulse at ~14,040 cal years BP (Figure 8A), probably as an extension of the previous oceanic conditions developed during the HE-I. During the B/A, it has been suggested that the ITCZ and NPH migrated northward (Pride et al., 1999). Our records in the northwestern GB (Hole U1545A) depict seasonal climatic conditions similar to those currently occurring when the NW winds are intense in the winter-spring, the GCW forms, and the productivity is high; while in summer, the SE winds are strong, and the TSW flows into the basin and the productivity in general is low. These conditions are consistent with previous studies (e.g., Barron et al., 2005; McClymont et al., 2012), in particular the latter study which suggested the alternation of periods of eutrophic and oligotrophic conditions with an increase in SST of 3°C recorded at ~13,000 cal years BP. In the central GB (Hole U1549A), the TSW increased. However, its occurrence is less evident (Figure 8D, 9B); this could be related to atmospheric modifications during the migration of the NPH, but more evidence is required.

4.3.3 Younger dryas (~12,800–11,600 cal years BP)

This period marks the glacial-to-interglacial transition that is characterized by ocean circulation changes. This study indicates that the CCW prevailed from ~12,700 to 11,800 cal years (Figures 8E, 9C) when the SST in the peninsular Pacific coast was estimated to be 5°C–6°C colder than in the Holocene (Rhode, 2002). This pattern could be related to the intensification of the CCS and CCW in the northeastern Pacific Ocean (Mix et al., 1999; Barron et al., 2003; Barron et al., 2005). At the end of the interval, from ~11,700 to 11,600 cal years BP (Figures 8G, 9E), our records suggest an increase in the formation of the GCW, which may be related to the increased ocean-land thermal contrast that resulted in the northward migration of the NPH and the intensification of NW winds (Cheshire and Thurow, 2013; Staines-Urías et al., 2015).

4.4 Holocene (~11,600 cal years BP to present)

From ~11,300 cal years BP to 640 cal years BP, our microfossil records show fluctuations of the TSW and GCW in the northwestern GB (Hole U1545A) (Figures 8D, G, 9B, E), dominated the TSW. Its occurrence in the GB has been significant since ~7,610 cal years BP, and the presence of GCW fluctuated at ~9,950, 7,310, 6,710, 5,120, 4,320, 3,950, and 2,710 cal years BP, and from ~1,000 to 490 cal years BP (Figure 8G). In the central GB (Hole U1549A), it is also suggested that the alternation of the TSW and GCW from ~11,500 to 133 cal years BP (Figures 8D, G, 9B, E) is more evident in the presence of tropical water during the Holocene. However, the records also indicate the presence of the GCW from ~10,900 to 6,030 cal years BP, and in several intervals from ~5,100 to 4,700, 4,150 to 3,000, 2,400 to 2,200, and from 480 to 130 cal years BP (Figure 8G). At the beginning of the Holocene, from ~11,600 to 6,000 cal years BP, incoming solar radiation at 23°N reached its maximum value (~450 W/m^2) (Figures 8C, 9A) (Berger and Loutre, 1991). Evidence indicates that a more northerly mean ITCZ latitude followed by gradual southern migrations (e.g., Barron et al., 2005; Koutavas and Lynch-Stieglitz, 2005) also marked this period. The ITCZ is manifested as a circum-global atmospheric belt of intense, moist convection and rainfall, marking the confluence of the northern and southern trade winds and the rising branch of the Hadley cell. In particular, the Holocene Climate Optimum (HCO), lasting from 10,000 to 6,000 cal years BP, is characterized by increased humidity and precipitation in low and mid-latitudes in the monsoon regions (Mayewski et al., 2004). In this period, the atmospheric polar cell contracted (Figures 7B, D) due to high insolation in the Northern Hemisphere (Figures 8C, 9A), and the influence of the Hadley and Ferrel cells increased (Figure 7D) (Cheshire and Thurow, 2013). This setting caused the intensification of the NW winds in the GB and the evaporation process, thus resulting in the GCW formation. From ~7,600 to

1,000 cal years BP, our records suggest a climatic monsoon regime alternating the TSW and the GCW (Figures 8D, G, 9B, E). These conditions coincide with a trend of warming of SST that occurred at 7,000 cal yr BP, which has been documented throughout the Eastern Tropical and Subtropical Pacific (Pahnke et al., 2007). Barron et al. (2012) identified warm SSTs in the central GoC between ~8,200 to 6,200 cal years BP and the modern monsoon onset at ~6,000 cal years BP (Barron et al., 2005; Pérez-Cruz, 2013). Warmer waters could be channeled northward along the axis of the GoC as gulf surges of monsoonal moisture (Bordoni and Stevens, 2006). During the modern summer–fall phase of the GoC, the NPH is located at ~ 35°N, the Northern Hemisphere insolation is at a maximum, and the ITCZ moves northward. From ~1,000 to 130 cal years BP, the occurrence of the GCW dominated in the GB. This condition may result from southward migration of the ITCZ mean annual position owing to decreasing insolation in the Northern Hemisphere during the boreal winter and the intensification of the NW winds and evaporation (Pérez-Cruz, 2013).

5 Conclusion

Analysis of siliceous microfossils, radiolarians and silicoflagellates, provides insights into changes in hydrographic structure, including water masses and circulation patterns during the last 31,000 cal years BP, contributing to the understanding of climatic and oceanographic conditions in the GoC, as well as the ETPO.

Major climatic periods are identified in GB cores: pre-Last Glacial Maximum time (~31,260–26,500 cal years BP), the Last Glacial Maximum (~26,500–19,000 cal years BP), the Heinrich-I event (~19,000–14,900 cal years BP), the Bølling-Ållerød (~14,900–12,800 cal years BP), the Younger Dryas (~12,800–11,600 cal years BP) and the Holocene (~11,600 to present). Short-term events linked to DO cycles are also observed.

The Pre-Last Glacial Maximum period was characterized by alternation of the CCW and GCW; and the occurrence of an extended PIW. The radiolarian assemblage represented by *C. davisiana* revealed the incursion of the CCW into the basin; the assemblage, including *Lithomelissa setosa* and *L. thoracites* showed the presence of GCW. We suggest that these conditions could be related to the amplification of the polar and subtropical jet streams, promoting the southern movement of the CCS and the incursion of CCW into the gulf. On the other hand, the dominance of *S. lineata* suggests a significant occurrence of the PIW due to more vigorous North Pacific Intermediate Water formation.

During the LGM, the radiolarian assemblage of surface dwellers such as *C. davisiana* and *B. aquilonaris*, as well as the silicoflagellate *Octactis speculum*, supports the incursion of the CCW into the basin, caused by the strengthening of the CCS, particularly from ~24,750 to 21,490 cal years BP. Radiolarian assemblage fluctuations during this period suggested that PIW was less evident from 23,500 to 21,240 cal years BP, possibly due to the weakening of NPIW formation. At the beginning (~26,000 cal years BP) and mainly at the end (~19,000 cal year BP) of LGM, PIW was dominant, which might be related to the formation and expansion of the NPIW.

The predominance of the PIW, indicated by the radiolarian assemblage at the beginning and end of this period, could be related to the formation and expansion of the NPIW. However, from 23,500 to 21,240 cal years BP, the PIW was less evident in the basin compared to the pre-LGM time, suggesting circulation changes influenced by the Pacific Ocean.

During the Heinrich-I event, we identified two major climatic conditions, beginning with the dominance of GCW-like waters owing to the weakened AMOC and the establishment of the PMOC, transporting saline waters northward and enhancing the occurrence of GCW-like conditions in the GB. During this interval, the PIW, along this interval, is related to the expanded formation of the NPIW and the occurrence of the CCW. These changes may be linked to the North Pacific oceanic circulation changes during the last glacial termination.

Our records suggest that the Bølling-Ållerød was a period with distinct hydrographic shifts related to the transition from glacial to interglacial conditions. Radiolarian assemblages and silicoflagellates suggested the alternated occurrence of three surface waters masses in the GB, referring to (1) the TSW as demonstrated by the assemblage of *T. octacantha* group and *P. pylonium* group, and the silicoflagellate *D. fibula* var. *messanensis*, (2) the GCW revealed by the radiolarian assemblages of *L. setosa*, *L. thoracites, P. longispinum*, and *Arachnochorallium calvata*, and the silicoflagellate *O. octonaria* var. *pulchra*, and (3) the episodic incursion of the CCW depicted by the radiolarian assemblage of *C. davisiana*, *B. aquilonaris*, *B. auritus australis* and the silicoflagellate *O. speculum*. These hydrographic conditions could be linked to the ITCZ's gradual northward migration and the NPH, and climatic conditions are likely to be similar to modern ones with a marked seasonality.

For the Younger Dryas, the radiolarian assemblage suggests the dominance of CCW. At the end of the interval, the formation of the GCW in the central GB, correlates to colder climatic conditions in the Northern Hemisphere and the strengthening of the CCS. On the other hand, the increased ocean-land thermal contrast and the gradual migration to the south of the NPH resulted in the intensification of NW winds and the formation of the GCW.

The TSW and the GCW alternate in the GB during the Holocene, and the modern climatic monsoon regime is identified from ~7,600 to 1,000 cal years BP. From ~1,000 to 130 cal years BP, the occurrence of the GCW suggests the southern latitudinal migration of the ITZC, the intensification of the NW winds, and the increase in evaporation processes.

Finally, throughout our records, we have identified episodic events, generally short-term, that suggest warm and cold climatic conditions that may be related to transitions between cold stadial (GS) and warmer interstadial (GI) conditions of the Dansgaard-Oeschger (D-O) events (GIs 6, 4 and 2, and GSs 6, 5, 4, and 3).

Data availability statement

The original contributions presented in the study are included in the article/Supplementary Material, further inquiries can be directed to the corresponding author.

Author contributions

MV-A: Formal Analysis, Investigation, Writing–original draft, Writing–review and editing. LP-C: Conceptualization, Investigation, Writing–original draft, Writing–review and editing. JU-F: Funding acquisition, Resources, Supervision, Writing–review and editing. KM: Methodology, Supervision, Writing–review and editing. EC-M: Supervision, Writing–review and editing. MM-G: Supervision, Writing–review and editing. AT: Writing–review and editing. TH: Investigation, Writing–review and editing. AA-C: Methodology, Software, Writing–review and editing. SJ: Writing–review and editing.

Funding

The author(s) declare financial support was received for the research, authorship, and/or publication of this article. This study was financially supported by the IICEAC Project 418908. LP-C acknowledges DGAPA PAPIIT, UNAM Project Number IN116623 for the partial financial support for this research.

Acknowledgments

This research used samples and data from the International Ocean Discovery Program (IODP). We thank the shipboard scientists, the IODP technical staff, and the R/V JOIDES Resolution crew for recovering the cores and for their invaluable assistance during the IODP Expedition 385. Mauricio Velázquez-Aguilar acknowledges the Posgrado en Ciencias del Mar y Limnología, UNAM, and the financial support provided by the Consejo Nacional de Humanidades, Ciencias y Tecnologías (CONAHCYT) for the PhD grant no. 762744. We greatly acknowledge the Editor, Teresa Drago, and journal reviewers, Fabienne Marret and Jonaotaro Onodera, for the detailed review and comments on the manuscript, which allowed us to improve it. We thank M.Sc Marysol Valdez-Hernández for her kind support of the creation and edition of the figures.

Conflict of interest

The authors declare that the research was conducted in the absence of any commercial or financial relationships that could be construed as a potential conflict of interest.

The author(s) declared that they were an editorial board member of Frontiers, at the time of submission. This had no impact on the peer review process and the final decision.

Publisher's note

All claims expressed in this article are solely those of the authors and do not necessarily represent those of their affiliated organizations, or those of the publisher, the editors and the reviewers. Any product that may be evaluated in this article, or claim that may be made by its manufacturer, is not guaranteed or endorsed by the publisher.

Supplementary material

The Supplementary Material for this article can be found online at: https://www.frontiersin.org/articles/10.3389/feart.2024.1301999/full#supplementary-material

References

Abelmann, A., and Gowing, M. M. (1997). Spatial distribution pattern of living polycystine radiolarian taxa-baseline study for paleoenvironmental reconstructions in the Southern Ocean (Atlantic Sector). *Mar. Micropaleontol.* 30, 3–28. doi:10.1016/S0377-8398(96)00021-7

Álvarez-Borrego, S. (2010). "Physical, chemical and biological oceanography of the Gulf of California," in *Gulf of California biodiversity and conservation*. Editor R. Brusca (Tucson: ASDM Press and University of Arizona Press), 22–48.

Álvarez-Borrego, S., and Lara-Lara, R. (1991). "The physical environment and primary productivity of the Gulf of California,". *The gulf and peninsular province of the californias*. Editors J. P. Dauphin and B. R. T. Simoneit (American Association of Petroleum Geologists, Memoir), 47, 555–567. doi:10.1306/M47542C26

Amador, J. A., Alfaro, E. J., Lizano, O. G., and Magaña, V. O. (2006). Atmospheric forcing of the Eastern tropical Pacific: a review. *Prog. Oceanogr.* 69, 101–142. doi:10.1016/j.pocean.2006.03.007

Andrews, J. T., and Dyke, A. S. (2007). "Late quaternary in north America,". *Encyclopedia of quaternary science*. Editor S. A. Elias (Amsterdam: Elsevier), v. 2, 1095–1101.

Badan-Dangon, A., Dorman, C. E., Merrifield, M. A., and Wianat, C. D. (1991). The lower atmosphere over the Gulf of California. *J. Geophys. Res.* 96 (9), 16877–16896. doi:10.1029/91JC01433

Bailey, J. W. (1856). Notice of microscopic forms found in the sounding of the Sea of kamtschatka. *Am. J. Sci. Arts*, 1–6. Second Series, 22, 64.

Barron, J. A., Bukry, D., and Bischoff, J. (2003). "A 2000-yr long record of climate from the Gulf of California," in *Proceedings of the nineteenth pacific climate workshop, asilomar, pacific grove, CA, march 3-6, 2002. Technical report 71, interagency ecological Program for the San Francisco estuary*. Editors G. J. West and N. L. Blomquist (Sacramento CA), 11–21.

Barron, J. A., Bukry, D., and Cheshire, H. (2014). Response of diatom and silicoflagellate assemblages in the central Gulf of California to regional climate change during the past 55 kyrs. *Mar. Micropaleontol.* 108, 28–40. doi:10.1016/j.marmicro.2014.02.004

Barron, J. A., Bukry, D., and Dean, W. E. (2005). Paleoceanographic history of the Guaymas Basin, Gulf of California, during the past 15,000 years based on diatoms, silicoflagellates, and biogenic sediments. *Mar. Micropaleontol.* 56, 81–102. doi:10.1016/j.marmicro.2005.04.001

Barron, J. A., Burky, D., and Bischoff, J. (2004). High resolution paleoceanography of the Guaymas Basin, Gulf of California, during the past 15 000 years. *Mar. Micropaleontol.* 50, 185–207. doi:10.1016/S0377-8398(03)00071-9

Barron, J. A., Metcalfe, S. E., and Addison, J. A. (2012). Response of the North American monsoon to regional changes in ocean surface temperature. *Paleoceanography* 27, PA3206. doi:10.1029/2011PA002235

Benson, R. N. (1966). Recent radiolaria from the gulf of California. Ph. D. Thesis, Minneapolis: University of Minnesota, 577.

Berger, A., and Loutre, M. F. (1991). Insolation values for the climate of the last 10 million years. *Quat. Sci. Rev.* 10 (4), 297–317. doi:10.1016/0277-3791(91)90033-Q

Bernal-Ramírez, R. (2003). Paleoceanografía reciente de alta resolución de los mares de Baja California Sur, México. Tesis de Doctorado. Mexico City, Mexico: Facultad de Ciencias, Universidad Nacional Autónoma de México, 121.

Björck, S., Walker, M. J. C., Cwynar, L. C., Johnsen, S., Knudsen, K.-L., Lowe, J. J., et al. (1998). An event stratigraphy for the Last Termination in the North Atlantic region based on the Greenland ice-core record: a proposal by the INTIMATE group. *J. Quat. Sci.* 13 (4), 283–292. members, intimate. doi:10.1002/(sici)1099-1417(199807/08)13:4<283::aid-jqs386>3.0.co;2-a

Blaauw, M., and Christen, J. A. (2011). Flexible paleoclimate age-depth models using an autoregressive gamma process. *Bayesian Anal.* 6 (3), 457–474. doi:10.1214/ba/1339616472

Boltovskoy, D., and Correa, N. (2016). Biogeography of radiolaria polycystina (protista) in the world ocean. *Prog. Oceanogr.* 149, 82–105. doi:10.1016/j.pocean.2016.09.006

Boltovskoy, D., Kling, S. A., Takahashi, K., and Bjorklund, K. (2010). World atlas of distribution of recent polycystina (Radiolaria). *Palaeontol. Electron.* 13 (3), 230.

Boltovskoy, D., and Riedel, W. R. (1987). Polycystine radiolaria of the California Current region: seasonal and geographic patterns. *Mar. Micropaleontol.* 12, 65–104. doi:10.1016/0377-8398(87)90014-4

Bordoni, S., and Stevens, B. (2006). Principal component analysis of the summertime winds over the Gulf of California: a Gulf surge index. *Mon. Weather Rev.* 134 (11), 3395–3414. doi:10.1175/MWR3253.1

Bray, N. A. (1988). Water mass formation in the Gulf of California. *J. Geophys. Res.* 93, 9223–9240. doi:10.1029/JC093iC08p09223

Castro, R., Collins, C. A., Rago, T. A., Margolina, T., and Navarro-Olache, L. F. (2017). Currents, transport, and thermohaline variability at the entrance of the Gulf of California (19-21 April 2013). *Ciencias Mar.* 43, 3. doi:10.7773/cm.v43i3.2771

Chang, F. H., Sutherland, J., and Bradford-Grieve, J. (2017). Taxonomic revision of Dictyochales (Dictyochophyceae) based on morphological, ultrastructural, biochemical and molecular data. *Phycol. Res.* 65 (3), 235–247. doi:10.1111/pre.12181

Cheshire, H., and Thurow, J. (2013). Novel approaches to a unifying hypothesis for the Northeast Pacific´s glacial mode of operation. *Paleoceanography* 28, 1–15. doi:10.1002/palo.20031

DeMenocal, P. B., Ortiz, J., Guilderson, T., and Sarnthein, M. (2000). Coherent high- and low-latitude climate variability during the Holocene warm period. *Science* 288, 2198–2202. doi:10.1126/science.288.5474.2198

Douglas, R., González-Yajimovich, O., Ledesma-Vázquez, J., and Staines-Urias, F. (2007). Climate forcing, primary production and the distribution of Holocene biogenic sediments in the Gulf of California. *Quat. Sci. Rev.* 26, 115–129. doi:10.1016/j.quascirev.2006.05.003

Ehrenberg, C. G. (1838). *Über die Bildung der Kriedefelsen und des Kriedemergels durch unsichtbare Organismen*. Ahandlungen: Königliche Akademie der Wissenshaften zu Berlin, 59–147.

Ehrenberg, C. G. (1862). Über die Tiefgrund-Verhältnisse des Oceans am Eingange der Davisstrasse und bei Island, Königliche Preussischen Akademie der Wissenschaften zu Berlín. Monatsbericht, 275–315.

Fatela, F., and Taborda, R. (2000). Confidence limits of species proportions in microfossil assemblages. *Mar. Micropaleontol.* 45, 169–174. doi:10.1016/S0377-8398(02)00021-X

Fernández-Barajas, M. E., Monreal-Gómez, M. A., and Molina-Cruz, A. (1994). Thermohaline structure and geostrophic flow in the Gulf of California, during 1992. *Ciencias Mar.* 20 (2), 267–286. doi:10.7773/cm.v20i2.958

García, H. E., Locarnini, R. A., Boyer, T. P., and Antonov, J. I. (2006). in *World Ocean atlas, 2005, dissolved oxygen, apparent oxygen utilization, and oxygen saturation, NOAA atlas*. Editor S. Levitus (Washington, D.C: U.S. Gov. Print. Off.), 3, 342. NESDIS 63.

Gong, X., Lembke-Jene, L., Lohmann, G., Knorr, G., Tiedemann, R., Zou, J. J., et al. (2019). Enhanced North Pacific deep-ocean stratification by stronger intermediate water formation during Heinrich Stadial 1. *Nat. Commun.* 10, 656. doi:10.1038/s41467-019-08606-2

Goodfriend, G. A., and Flessa, K. W. (1997). Radiocarbon reservoir ages in the Gulf of California: roles of upwelling and flow from the Colorado River. *Radiocarbon* 39, 139–148. doi:10.1017/S0033822200051985

Guiry, M. D., and Guiry, G. M. (2023). *AlgaeBase. World-wide electronic publication*. Galway, Ireland: National University of Ireland. Available at: http://www.algaebase.org.

Haeckel, E. (1862). *DieRadiolarien (rhizopoda, radiolaria), eine monographie*. Berlin: Reimer, 1–572.

Haeckel, E. (1887). Report on the radiolaria collected by HMS "challenger" during the years 1873-1876. *Rep. Sci. Results, Voyage HMS Chall. Zool.* 18, 1–1803.

Heaton, T., Köhler, P., Butzin, M., Bard, E., Reimer, R., Austin, W., et al. (2020). Marine20 - the marine radiocarbon age calibration curve (0-55,000 cal BP). *Radiocarbon* 62, 779–820. doi:10.1017/RDC.2020.68

Hirama, M. V., Toledo, F. A. L., Camillo, E., Badaraco-Costa, K., and Pereira-de-Cuadros, J. (2010). Q-mode and R-mode factor analysis in quantitative studies of microfossils of the Late Quaternary in sediments from the Brazilian continental margin. *Sci. Commun. Terrae* 7 (1-2), 41–49.

Hu, W. F., Zhang, L. L., Chen, M. H., Zeng, L. L., Zhou, W. H., Xiang, R., et al. (2015). Distribution of living radiolarians in spring in the South China Sea and its responses to environmental factors. *Sci. China Earth Sci.* 58, 270–285. doi:10.1007/s11430-014-4950-0

Hughes, P. D., Gibbard, P. L., and Ehlers, J. (2013). Timing of glaciation during the last glacial cycle: evaluating the concept of a global "Last Glacial Maximum" (LGM). *Earth-Science Rev.* 125, 171–198. doi:10.1016/j.earscirev.2013.07.003

Ishitani, Y., and Takahashi, K. (2007). The vertical distribution of Radiolaria in the waters surrounding Japan. *Mar. Micropaleontol.* 65, 113–136. doi:10.1016/j.marmicro.2007.06.002

Jorgensen, E. (1900). Protophyten und Protozöen in Plankton aus der norwegischen Westküste. *Bergens Mus. Aarb.* 6, 51–112.

Jull, J. T. A. (2007). "Radiocarbon dating. AMS method," in *Encyclopedia of quaternary science*. Editor A. E Scott. 1st edicion (Elsevier Science), 2911–2918.

Keiwing, L., and Jones, G. (1990). Deglacial climatic oscillations in the gulf of California. *Paleoceanography* 5 (6), 1009–1023. doi:10.1029/PA005i006p01009

Kessler, W. S. (2006). The circulation of the eastern tropical Pacific: a review. *Prog. Oceanogr.* 69, 181–217. doi:10.1016/j.pocean.2006.03.009

Kling, S. A. (1979). Vertical distribution of polycystine radiolarians in the central North Pacific. *Mar. Micropaleontol.* 4, 295–318. doi:10.1016/0377-8398(79)90022-7

Kling, S. A., and Boltovskoy, D. (1995). Radiolarian vertical distribution patterns across the southern California Current. *Deep-Sea Res. I* 42 (2), 191–231. doi:10.1016/0967-0637(94)00038-T

Koutavas, A., and Lynch-Stieglitz, J. (2005). "Variability of the marine ITCZ over the eastern pacific during the past 30,000 years. Regional perspective and global context," in *The Hadley circulation: present past and future*. Editors H. F. Diaz and R. S. Bradley (Springer Academic Publishers), 347–369.

Lavín, M. F., Castro, R., Beier, E., Cabrera-Ramos, C. E., Godínez, V. M., and Amador-Buenrostro, A. (2014). Surface circulation in the Gulf of California in summer from surface drifters and satellite images (2004-2006). *J. Geophys. Research-Oceans* 119, 4278–4290. doi:10.1002/2013jc009345

Lavin, M. F., Castro, R., Beier, E., Godínez, V. M., Amador, A., and Guest, P. (2009). SST, thermohaline structure, and circulation in the southern gulf of California in june 2004 during the North American monsoon experiment. *J. Geophys. Res.*, 114, C02025, 22 p. doi:10.1029/2008JC004896

Lavin, M. F., and Marinone, S. G. (2003). "An overview of the physical oceanography of the Gulf of California," in *Nonlinear processes in geophysical fluid dynamics*. Editor O. U. Velasco-Fuentes (Netherlands: Kluwer Academic Publishers), 173–204.

Lemmerman, E. (1901). Silicoflagellatae: ergebnisse einer Reise nach dem. *Dtsch. Bot. Ges.* 19 (1901), 247–271.

Lizarralde, D., Axen, G. J., Brown, H. E., Fletcher, J. M., González-Fernández, A., Harding, A. J., et al. (2007). Variation in styles of rifting in the Gulf of California. *Nature* 448 (7152), 466–469. doi:10.1038/nature06035

Loubere, P., and Qian, H. (1997). Reconstructing Paleoecology and paleoenvironmental variables using factor analysis and regression: some limitations. *Mar. Micropaleontol.* 31, 205–217. doi:10.1016/S0377-8398(97)00002-9

Lüer, V., Hollis, C. J., and Willems, H. (2008). Late Quaternary radiolarian assemblages as indicators of paleoceanographic changes north of the subtropical front, offshore eastern New Zealand, southwest Pacific. *Micropaleontology* 54 (1), 49–69. doi:10.47894/mpal.54.1.06

MARGO project members (2009). Constraints on the magnitude and patterns of ocean cooling at the Last Glacial Maximum. *Nat. Geosci.* 2, 127–132. doi:10.1038/ngeo411

Marinone, S. G. (2003). A three-dimensional model of the mean and seasonal circulation of the Gulf of California. *J. Geophys. Res.* 108, 3325. C10. doi:10.1029/2002JC001720

Matul, A., Barash, M., Khusid, T. A., Behera, P., and Tiwari, M. (2018). Paleoenvironment variability during termination I at the reykjanes ridge, north atlantic. *Geosciences* 8, 375. doi:10.3390/geosciences8100375

Matul, A., and Mohan, R. (2017). Distribution of polycystine radiolarians in bottom surface sediments and its relation to summer sea temperature in the high-latitude north atlantic. *Front. Mar. Sci.* 4, 330. doi:10.3389/fmars.2017.00330

Mayewski, P. A., Rohlingb, E. E., Stagerc, J. C., Karlén, W., Maascha, K. A., Meekere, L. D., et al. (2004). Holocene climate variability. *Quat. Res.* 62, 2434–3255. doi:10.1016/j.yqres.2004.07.001

McClymont, E., Ganeshram, R., Pichevin, L., Talbot, H., Dongen, B., Thunell, R., et al. (2012). Sea-surface temperature records of Termination 1 in the Gulf of California: challenges for seasonal and interannual analogues of tropical Pacific climate change. *Paleoceanography* 27, 1–15. doi:10.1029/2011PA002226

McManus, J. F., Francois, R., Gherardi, J. M., Keigwin, L. D., and Brown-Leger, S. (2004). Collapse and rapid resumption of Atlantic meridional circulation linked to deglacial climate changes. *Nature* 428, 834–837. doi:10.1038/nature02494

Miller, N., and Lizarralde, D. (2013). Thick evaporites and early rifting in the Guaymas Basin, gulf of California. *Geology* 41 (2), 283–286. doi:10.1130/G33747.1

Mix, A. C., Lund, D. C., Pisias, N. G., Boden, P., Bornmalm, L., Lyle, M., et al. (1999). "Rapid climate oscillations in the Northeast Pacific during the last deglaciation reflect northern and southern hemisphere sources," in *Mechanisms of global climate change at millennial time scales, AGU monograph 112*. Editors P. U. Clark, R. S. Webb, and L. D. Keigwin (Washington DC: American Geophysical Union), 127–148.

Molina-Cruz, A. (1986). Evolución oceanográfica de la boca del Golfo de California. *An. del Inst. Ciencias del Mar Limnol. UNAM* 13 (2), 95–120.

Molina-Cruz, A., Welling, L. A., and Caudillo-Bohorquez, A. (1999). Radiolarian distribution in the water column, southern Gulf of California, and its implication in thanatocoenose constitution. *Mar. Micropaleontol.* 37 (2), 149–171. doi:10.1016/S0377-8398(99)00030-4

Morley, J. J. (1980). Analysis of the abundance variations of the subspecies of Cycladophora davisiana. *Mar. Micropaleontol.* 5, 205–214. doi:10.1016/0377-8398(80)90011-0

Müller, J. (1858). *Über die Thalassicollen, Polycistinen und Acanthometren des Mittelmeeres*. Abhandlungen: Königliche Akademie Wissenschaften Berlin, 1–62.

Murray, D., and Schrader, H. (1983). Distribution of silicoflagellates in plankton and core top samples from the gulf of California. *Mar. Micropaleontol.* 7, 517–539. doi:10.1016/0377-8398(83)90013-0

Nigrini, C. (1977). Tropical cenozoic artostrobiidae (radiolaria). *Micropaleontology* 23, 241–269. doi:10.2307/1485215

Nimmergut, A., and Abelmann, A. (2002). Spatial and seasonal changes of radiolarian standing stocks in the Sea of Okhotsk. *Deep Sea Res. I* 49, 463–493. doi:10.1016/s0967-0637(01)00074-7

Okazaki, Y., Takahashi, K., Nakatsuka, T., and Honda, M. C. (2003). The production scheme of Cycladophora davisiana (Radiolaria) in the Okhotsk Sea and the northwestern North Pacific: implication for the paleoceanographic conditions during the glacials in the high latitude oceans. *Geophys. Res.* 30 (18). doi:10.1029/2003GL018070

Okazaki, Y., Timmermann, A., Mneviel, L., Chikamoto, M. O., Harada, N., and Abe-Ouchi, A. (2012). Ocean circulation in the North Pacific during the last glacial termination. *PAGES News* 20-2, 60–61. doi:10.22498/pages.20.2.60

Onodera, J., and Takahashi, K. (2005). Silicoflagellate fluxes and environmental variations in the northwestern North Pacific during december 1997–may 2000. *Deep-Sea Res. I* 52, 371–388. doi:10.1016/j.dsr.2004.10.001

Ortiz, J. D. (2011). Application of visible/near infrared derivative spectroscopy to arctic paleoceanography. *IOP Conf. Ser. Earth Environ. Sci.* 14, 012011. doi:10.1088/1755-1315/14/1/012011

Pahnke, K., Sachs, J. P., Keigwin, L., Timmermann, A., and Xie, S. P. (2007). Eastern tropical Pacific hydrologic changes during the past 27,000 years from D/H ratios in alkenones. *Paleoceanography* 22, PA4214. doi:10.1029/2007pa001468

Pérez-Cruz, L. (2006). Climate and ocean variability during the middle and late Holocene recorded in laminated sediments from Alfonso Basin, Gulf of California, México. *Quat. Res.* 65, 401–410. doi:10.1016/j.yqres.2006.02.003

Pérez-Cruz, L. (2013). Hydrological changes and paleoproductivity in the Gulf of California during middle and late Holocene and their relationship with ITCZ and North American Monsoon variability. *Quat. Res.* 79, 138–151. doi:10.1016/j.yqres.2012.11.007

Pérez-Cruz, L., and Molina-Cruz, A. (1988). El Niño 1983: effect on the distribution of the silicoflagelados in the gulf of California. *Ciencias Mar.* 14 (3), 9–38. doi:10.7773/cm.v14i3.606

Petrushevskaya, M. G. (1971). "Radiolaria in the plankton and recents sediments from the Indian ocean and Anthartic," in *The micropaleontology of oceans*. Editors B. M. Funnell and W. R. Riedel (Cambridge: Cambridge University press), 319–329.

Pichevin, L., Ganeshram, R. S., Reynolds, B. C., Prahl, F., Pedersen, T. F., Thunell, R., et al. (2012). Silicic acid biogeochemistry in the Gulf of California: insights from sedimentary Si isotopes. *Paleoceanography*, 27, PA 2201. doi:10.1029/2011PA002237

Pisias, N. G. (1986). Vertical water mass circulation and the distribution of radiolaria in surface sediments of the gulf of California. *Mar. Micropaleontol.* 10, 189–205. doi:10.1016/0377-8398(86)90029-0

Pisias, N. G., Murray, G. R., and Scudder, R. P. (2013). Multivariate statistical analysis and partitioning of sedimentary geochemical data sets: general principles and specific MATLAB scripts. *Geochem. Geophys. Geosystems* 14, 4015–4020. doi:10.1002/ggge.20247

Portela, E., Beier, E., Barton, E. D., Castro, R., Godínez, V., Palacios-Hernández, E., et al. (2016). Water masses and circulation in the tropical pacific off Central Mexico and surrounding areas. *J. Phys. Oceanogr. Am. Meteorological Soc.* 46, 3069–3081. doi:10.1175/JPO-D-16-0068.1

Price, A. M., Kenneth, N. M., Vera, P., Thomas, F. P., and Ganeshram, R. (2012). Late quaternary climatic and oceanographic changes in the northeast pacific as recorded by dinoflagellate cysts from Guaymas Basin, gulf of California (Mexico). *Paleoceanography* 28, 200–212. doi:10.1002/palo.20019

Pride, C., Thunell, R., Sigman, D., Keigwin, L., Altabet, M., and Tappa, E. (1999). Nitrogen isotopic variations in the Gulf of California since the Last Deglaciation: response to global climate change. *Paleoceanography* 14, 397–409. doi:10.1029/1999pa900004

R Core Team (2023). *R: a language and environment for statistical computing*. Vienna, Austria: R Foundation for Statistical Computing. Version 4.3.0. Available at: https://www.R-project.org/.

Rhode, D. (2002). Early Holocene juniper woodland and chaparral taxa in the central Baja California peninsula, Mexico. *Quat. Res.* 57, 102–108. doi:10.1006/qres.2001.2287

Roden, G. I. (1964). "Oceanographic aspects of the gulf of California," in *Marine geology of the gulf of California*. Editors T. van Andel. and G. G. Shor (OK, United States: Am. Assoc. Petrol. Geol. Mem.), 3, 30–58.

Sancetta, C. (1995). Diatoms in the Gulf of California: seasonal flux patterns and the sediment record for the last 15,000 years. *Paleoceanography* 10, 67–84. doi:10.1029/94pa02796

Schneider, T., Bischoff, T., and Haug, G. (2014). Migrations and dynamics of the intertropical convergence zone. *Nature* 513, 45–53. doi:10.1038/nature13636

Schrader, H., and Murray, D. (1985). Silicoflagellate assemblages in the Gulf of California during the last glacial maximum and the present: oceanographic implications. *Mar. Micropaleontol.* 9, 18228.

Schrader, H., Pisias, N., and Cheng, G. (1986). Seasonal variation of silicoflagellates in phytoplankton and varved sediments in the Gulf of California. *Mar. Micropaleontol.* 10 (1–3), 207–233. doi:10.1016/0377-8398(86)90030-7

Staines-Urías, F., Gónzalez-Yajimovich, O., and Beaufort, L. (2015). Reconstruction of past climate variability and ENSO-like fluctuations in the Southern Gulf of California (Alfonso Basin) since the last glacial maximum. *Quat. Res.* 83, 488–501. doi:10.1016/j.yqres.2015.03.007

Stock, J. M., and Hodges, K. V. (1989). Pre-Pliocene extension around the Gulf of California and the transfer of Baja California to the Pacific plate. *Tectonics* 8, 99–115. doi:10.1029/tc008i001p00099

Takahashi, K. (1987). Radiolarian flux and seasonality: climatic and El Niño response in the subarctic Pacific, 1982-1984. *Glob. Biogeochem. Cycles* 1 (3), 213–231. doi:10.1029/GB001i003p00213

Takahashi, K. (1991). Radiolaria: flux, ecology, and taxonomy in the pacific and atlantic ocean biocenosis, woods hole oceanographic institution (Massachusetts). *Series* 3, 1–303. doi:10.1575/1912/408

Tanaka, S., and Takahashi, K. (2008). Detailed vertical distribution of radiolarian assemblage (0-3000 m, fifteen layers) in the central subarctic Pacific, June 2006. *Mem. Fac. Sci., Kyushu Univ., Ser. D, Earth Planet. Sci.* 32 (1), 49–72. doi:10.5109/11807

Teske, A., Lizarralde, D., Höfig, T. W., Aiello, I. W., Ash, J. L., Bojanova, D. P., et al. (2021a). "The expedition 385 scientists, Guaymas Basin tectonics and biosphere," in Proceedings of the International Ocean Discovery Program. Editors A. Teske, D. Lizarralde, and T. W. Höfig (College Station, TX: International Ocean Discovery Program), 385. Site U1545. doi:10.14379/iodp.proc.385.106.2021

Teske, A., McKay, L. J., Ravelo, A. C., Aiello, I., Mortera, C., Núñez-Useche, F., et al. (2019). Characteristics and evolution of sill-driven off-axis hydrothermalism in Guaymas Basin – the ringvent site. *Sci. Rep.* 9, 13847. doi:10.1038/s41598-019-50200-5

Teske, P. A., Lizarralde, D., and Höfig, T. (2020). International Ocean Discovery Program expedition 385 preliminary report Guaymas Basin tectonics and biosphere. IODP & the Expedition 385 Scientists.

Teske, P. A., Lizarralde, D., Höfig, T. W., Aiello, I. W., Ash, J. L., Bojanova, D. P., et al. (2021b). "The expedition 385 scientists, Guaymas Basin tectonics and biosphere," in Proceedings of the International Ocean Discovery Program. Editors A. Teske, D. Lizarralde, and T. W. Höfig (College Station, TX: International Ocean Discovery Program), 385. Site U1549. doi:10.14379/iodp.proc.385.103.2021

Welling, L. A., and Pisias, N. G. (1993). Seasonal trends and preservation biases of polycystine radiolaria in the northern California current system. *Paleoceanography* 8, 351–372. doi:10.1029/93pa00384

Welling, L. A., Pisias, N. G., Johnson, E. S., and White, J. R. (1996). Distribution of polycystine radiolaria and their relation to the physical environment during the 1992 El Niño and following cold event. *Deep-Sea Res. II* 43, 1413–1434. doi:10.1016/0967-0645(96)00013-6

Yamashita, H., Takahashi, K., and Fujitani, N. (2002). Zonal and vertical distribution of radiolarians in the western and central Equatorial Pacific in January 1999. *Deep-Sea Res. II* 49, 2823–2862. doi:10.1016/s0967-0645(02)00060-7